

THESIS

A CELLULAR PRION PROTEIN-DEPENDENT SIGNALING PATHWAY FOR  
PROINFLAMMATORY CYTOKINE- AND  $\beta$ -AMYLOID-INDUCED COFILIN-ACTIN ROD  
FORMATION

Submitted by

Keifer P. Walsh

Graduate Degree Program in Cell and Molecular Biology

In partial fulfillment of the requirements

For the Degree of Master of Science

Colorado State University

Fort Collins, Colorado

Fall 2014

Master's Committee:

Advisor: James Bamberg

Mark Zabel  
Ron Tjalkens

Copyright by Keifer Patrick Walsh 2014

All Rights Reserved

## ABSTRACT

### A CELLULAR PRION PROTEIN-DEPENDENT SIGNALING PATHWAY FOR PROINFLAMMATORY CYTOKINE- AND $\beta$ -AMYLOID-INDUCED COFILIN-ACTIN ROD FORMATION

Stimulus of oxidative stress in neurodegeneration leads to synaptic dysfunction and the eventual loss of neurons in the central nervous system. The actin cytoskeleton of neurons under acute or chronic stress experiences dynamic remodeling due to functional alterations in the actin depolymerizing factor (ADF)/cofilin family of actin-binding proteins. Once oxidized, disulfide cross-linked cofilin incorporates into the formation of tandem arrays of 1:1 cofilin:actin rod-like bundles (rods). Rods sequester cofilin, which is required for synaptic remodeling associated with learning and memory, and interrupt vesicular transport by occluding the neurite within which they form.

Different rod-inducing stimuli target distinct neuronal populations within the hippocampus. Rods form rapidly (5-30 min) in >80% of cultured hippocampal neurons which are treated with excitotoxic levels of glutamate or energy depleted (hypoxia/ischemia or mitochondrial inhibitors). In contrast, slow rod formation (50% maximum response in ~6 h) occurs in ~20% of neurons upon exposure to soluble beta-amyloid dimer/trimer ( $A\beta$ d/t), a physiologically relevant species in Alzheimer disease (AD). Here we show that proinflammatory cytokines ( $TNF\alpha$ ,  $IL-1\beta$ ,  $IL-6$ ) induce rods at the same rate and in the same subpopulation of hippocampal neurons that respond to  $A\beta$ d/t. Rod formation by proinflammatory cytokines may link the neuroinflammatory

hypothesis for AD with the A $\beta$  hypothesis by providing a common target. Neurons from PrP<sup>C</sup>-null mice form rods in response to glutamate or antimycin A, but not in response to A $\beta$ d/t or proinflammatory cytokines. Prion-dependent rod inducers require the activation of NADPH oxidase (NOX) to generate reactive oxygen species (ROS), but NOX activity is not required for rods induced by glutamate or energy depletion.

A $\beta$ d/t and TNF $\alpha$  stimulate cofilin dephosphorylation and increased ROS production in a subpopulation of neurites at levels that exceed a minimum threshold to maintain stable rods. Removing inducers or inhibiting NOX activity in cells containing prion-dependent rods causes rod disappearance with a half-life of ~36 minutes. Interestingly, the overexpression of PrP<sup>C</sup> alone is sufficient to induce rods in >40% of hippocampal neurons, nearly twice the number that respond to A $\beta$ d/t or TNF $\alpha$ . This suggests that membrane microdomains containing PrP<sup>C</sup> recruit the oxidizing machinery necessary to initiate and sustain rod formation. Our hypothesis is supported by the inhibition and reversal of prion-dependent rods by the naturally occurring plant triterpene, ursolic acid (UA), and the pharmacological peptide RAP310. UA and related compounds to RAP310 have been proposed to inhibit changes in the membrane lipid profile that permit LR coalescence.

The vast majority of neurodegenerative disorders are considered sporadic in incidence and multifactorial in cause, making treatment at an early stage a significant challenge. If cofilin-actin rods indeed bridge multiple disease initiating mechanisms into a common pathway leading to synapse loss, they provide a valuable target for therapeutic intervention.

## ACKNOWLEDGEMENTS

I would like to acknowledge my advisor, Dr. James Bamburg, for his profound guidance, unrelenting patience, and above all, for the opportunity to contribute to his research field. I would like to thank my committee members Dr. Mark Zabel and Dr. Ron Tjalkens for their comments and suggestions in my preparation of this thesis and Dr. Zabel for his collaborations in providing PrP<sup>C</sup>-null mice. Dr. Thomas Kuhn played a pivotal role in my development as researcher, as well as initially suggesting a possible cytokine mechanism for rod formation and providing a supply of ursolic acid, for all of which I am greatly appreciative. I also want to thank Dr. David Lambeth, Emory University, for sharing with us his (at the time unpublished) NOX inhibitors.

In my years of research experience, I was very fortunate to be surrounded by many great minds, an invaluable resource to my success. I am grateful for the advice and assistance of my other laboratory members Laurie Minamide, Dr. O'Neil Wiggan, Alisa Shaw, Dr. Barbara Bernstein, Ian Marsden, Jianje Mi, Sarah Kane, and Adlei Carlson. I would also like to recognize Dan Peacock and Lindsey Whittington for their help in live imaging and analysis.

Finally, I would like to dedicate this work to those affected by Alzheimer disease. My grandmother's diagnosis fueled my interest in research, upon which I found Dr. Bamburg's work and made initial contact through the CSU Honors Undergraduate Research Scholars program in my senior year of high school. My five years in the research field has given me great confidence because of the brilliant, driven, and compassionate individuals with whom I have had the opportunity to work.

## TABLE OF CONTENTS

ABSTRACT .....	ii
ACKNOWLEDGEMENTS .....	iv
TABLE OF CONTENTS .....	v
LIST OF FIGURES.....	viii
LIST OF ABBREVIATIONS.....	xi
CHAPTER 1: INTRODUCTION.....	1
<b>Neurodegenerative Disorders and <math>\beta</math>-Amyloid</b> .....	1
<b>ADF/Cofilin-Actin Rod Formation</b> .....	4
<b>Proposal for Two Independent Pathways for Rod Formation</b> .....	11
CHAPTER 2: PROINFLAMMATORY CYTOKINES AND $\beta$ -AMYLOID INDUCE COFILIN-ACTIN ROD FORMATION.....	14
<b>Introduction</b> .....	14
<b>Materials and Methods</b> .....	15
<b>Results</b> .....	22
<i>CofilinR21Q-mRFP functions as a rod reporter for real time           imaging</i> .....	22
<i>Proinflammatory cytokines induce cofilin-actin rods</i> .....	22
<i>TNF<math>\alpha</math> and A<math>\beta</math>d/t target the same population of hippocampal           neurons</i> .....	25
<i>TNF<math>\alpha</math> initiates cofilin dephosphorylation</i> .....	25

<i>Rod persistence requires the presence of inducing agent</i> .....	27
<b>Discussion</b> .....	29
 CHAPTER 3: A CELLULAR PRION PROTEIN-DEPENDENT SIGNALING PATHWAY FOR NADPH OXIDASE ACTIVATION.....	
	32
<b>Introduction</b> .....	32
<b>Materials and Methods</b> .....	35
<b>Results</b> .....	38
<i>PrP<sup>C</sup> is required for A<math>\beta</math>d/t, TNF<math>\alpha</math>, IL-1<math>\beta</math> &amp; IL-6-induced rods</i> .....	38
<i>PrP<sup>C</sup> overexpression is sufficient for rod formation</i> .....	40
<i>NOX inhibition prevents A<math>\beta</math>d/t- and TNF<math>\alpha</math>-induced rod formation</i> .....	46
<i>A<math>\beta</math>d/t and TNF<math>\alpha</math> stimulate ROS generation in neurites</i> .....	49
<i>NOX inhibition reverses prion-dependent rods</i> .....	51
<b>Discussion</b> .....	54
 CHAPTER 4: URSOLIC ACID AND RAP310 INHIBIT AND REVERSE PRION- DEPENDENT ROD FORMATION.....	
	57
<b>Introduction</b> .....	57
<b>Materials and Methods</b> .....	59
<b>Results</b> .....	60
<i>UA inhibits and reverses A<math>\beta</math>d/t- and TNF<math>\alpha</math>-induced rods</i> .....	60
<i>RAP310 inhibits and reverses A<math>\beta</math>d/t- and TNF<math>\alpha</math>-induced rods</i> .....	60
<i>Reversal of A<math>\beta</math>d/t- and TNF<math>\alpha</math>-stimulated ROS production by UA         and RAP310</i> .....	61
<i>Reversal of prion-dependent rods by UA and RAP310</i> .....	64

<b>Discussion .....</b>	<b>64</b>
CHAPTER 5: CONCLUSIONS AND FUTURE DIRECTIONS .....	69
REFERENCES.....	71

## LIST OF FIGURES

Figure 1.1	APP proteolytic processing.....	3
Figure 1.2	Tau hyperphosphorylation and microtubule destabilization.....	5
Figure 1.3	ADF/cofilin regulates actin dynamics.....	7
Figure 1.4	Cofilin-actin rods occlude the entire neurite, obstructing vesicular transport .....	8
Figure 1.5	Circuitry of the hippocampus: dentate gyrus and cornu ammonis .....	10
Figure 1.6	Schematic model of a prion-mediated signaling mechanism for rod formation .....	13
Figure 2.1	CofilinR21Q-mRFP is a genetically encoded rod reporter.....	16
Figure 2.2	CofilinR21Q-mRFP rods in live cell imaging.....	23
Figure 2.3	Proinflammatory cytokine dose-response curves and time course of rod formation in dissociated hippocampal neurons .....	24
Figure 2.4	Rod formation in neurons in response to A $\beta$ d/t and TNF $\alpha$ used separately or together and their reversibility 24 h after washout.....	26
Figure 2.5	TNF $\alpha$ induces cofilin activation within neurites in which rods form but not in other neurites or neurons .....	28
Figure 2.6	Rod dynamics and reversal observed in neurons using live cell	

imaging.....	30
Figure 3.1 Secondary structure and interactions of the cellular prion protein.....	33
Figure 3.2 Neuronal NOX isoforms and assembly .....	36
Figure 3.3 CTxB-stained lipid rafts.....	39
Figure 3.4 PrP <sup>C</sup> is required for rod formation from A $\beta$ d/t and proinflammatory cytokines, but not from rods induced by glutamate or mitochondrial inhibitors.....	41
Figure 3.5 PrP <sup>C</sup> overexpression induces rods in both rat and mouse neurons and requires NOX for rod formation .....	43
Figure 3.6 Cofilin-actin rod formation co-localizes with distinct PrP <sup>C</sup> patches.....	45
Figure 3.7 NOX-1/2 immunoblots .....	47
Figure 3.8 A $\beta$ d/t and TNF $\alpha$ utilize a NOX-dependent pathway for rod formation.....	48
Figure 3.9 DCF analysis for measurement of ROS production .....	50
Figure 3.10 A $\beta$ d/t and TNF $\alpha$ initiate the generation of ROS in neurites .....	52
Figure 3.11 Prion-dependent rod reversibility upon NOX inhibition.....	53
Figure 4.1 Triterpenoid structure (UA).....	58

Figure 4.2	UA inhibits and reverses A $\beta$ d/t- and TNF $\alpha$ -induced rods .....	62
Figure 4.3	RAP310 inhibits and reverses A $\beta$ d/t- and TNF $\alpha$ -induced rods.....	63
Figure 4.4	UA and RAP310 reverse A $\beta$ d/t- and TNF $\alpha$ -induced ROS production .....	65
Figure 4.5	UA and RAP310 reverse rods induced by PrP <sup>C</sup> overexpression.....	66

## LIST OF ABBREVIATIONS

A $\beta$ d/t	Beta-amyloid dimer/trimer
AD	Alzheimer disease
ADF	Actin depolymerizing factor
APP	Amyloid precursor protein
CJD	Creutzfeldt-Jakob disease
CNS	Central nervous system
CTE	Chronic traumatic encephalopathy
CTxB	Cholera toxin B subunit
CWD	Chronic wasting disease
DAPTA	D-ala-peptide T-amide (Peptide T)
DG	Dentate gyrus of the hippocampus
EGFP	Enhanced green fluorescent protein
GPI	Glycophosphatidylinositol
IL	Interleukin (-1 $\beta$ , -6)
LR	Lipid raft
LTP	Long-term potentiation
mGluR	Metabotropic glutamate receptor
mRFP	Monomeric red fluorescent protein
MT	Microtubule
NFT	Neurofibrillary tangle
NMDA	N-methyl-D-aspartate
NOX	NADPH oxidase
PIP <sub>2</sub>	Phosphatidyl inositol 4,5-bisphosphate
PrP <sup>C</sup>	Cellular prion protein
PrP <sup>Sc</sup>	Infectious (scrapie) prion protein
RAP310	Rapid Pharmaceuticals, AG peptide "310"
ROS	Reactive oxygen species
SSH	Slingshot
TACE	TNF $\alpha$ converting enzyme
TBI	Traumatic brain injury (mTBI, mild)
TIRF	Total internal reflection fluorescence
TNF $\alpha$	Tumor necrosis factor-alpha
UA	Ursolic acid

## CHAPTER 1: INTRODUCTION

### **Neurodegenerative Disorders and $\beta$ -Amyloid**

Most neurodegenerative disorders are age-dependent as their incidence increases with advancing age. A mounting body of evidence argues that many of these disorders are caused by prions, or misfolded counterparts of otherwise normal proteins. The conversion of cellular prion protein ( $\text{PrP}^{\text{C}}$ ) to the infectious scrapie  $\text{PrP}^{\text{Sc}}$  is fundamental to the onset of various prionopathies that include Creutzfeldt-Jakob disease (CJD) in humans, scrapie in sheep, chronic wasting disease (CWD) in deer and elk, and mad cow disease (Prusiner, 2013). Likewise, beta-amyloid ( $\text{A}\beta$ ), tau,  $\alpha$ -synuclein, and possibly huntingtin fall under this prion-like classification and cause distinct neurodegenerative diseases.

The role of a neuroinflammatory response in traumatic brain injuries (TBI) and other neurodegenerative disorders, e.g. Alzheimer, Parkinson, and Huntington diseases, is being actively investigated (Cacquevel *et al.*, 2004; Möller, 2010; Amor *et al.*, 2010, 2014; Liu & Chan, 2014). A unique class of neuroinflammatory disorders has gained prominence recently in various sports and has sparked a national debate about both the safety of players and the responsibilities of national sports organizations. Repetitive mild TBIs (mTBI), such as concussion and subconcussion, can lead to the development of chronic traumatic encephalopathy (CTE) and produce persistent cognitive, behavioral, and psychiatric problems (McKee *et al.*, 2014). Proinflammatory cytokines, including tumor necrosis factor alpha ( $\text{TNF}\alpha$ ) and interleukins ( $\text{IL}$ )- $1\beta$  and  $\text{IL}$ -6 are increased in

mTBI (Briones *et al.*, 2013; Yang *et al.*, 2013; Ferreira *et al.*, 2013) and modulate deficits in motor coordination (Longhi *et al.*, 2013).

Alzheimer disease (AD) is among the age-related neurodegenerative disorders often associated with neuroinflammation (Cacquevel *et al.*, 2004; Liu & Chan, 2014). AD and other dementia-related diseases place an immense financial and emotional burden on families of those affected. According to a comprehensive report by the Alzheimer Association, AD is the sixth leading cause of all deaths in the United States, costing an estimated \$214 billion in 2014, and demanding nearly one in every five dollars of Medicare spending for providing care. The number of diagnosed individuals is expected to nearly triple by 2050. At the time of the report, the U.S. Food and Drug Administration had approved five drugs to temporarily slow symptoms for 6-12 months, on average, that work for about half of the individuals who take them, the last of which was approved in 2003. In addition to these approved drugs, evidence suggests that management of cardiovascular risk factors (Luchsinger & Mayeux, 2004), along with regular physical exercise, a diet rich in fruits and vegetables (Miller & Shukitt-Hale, 2012), a robust social network, and diverse mental stimulation (Wilson *et al.*, 2002) may aid in slowing the onset of AD-related symptoms.

Senile plaques composed of beta-amyloid (A $\beta$ ) and neurofibrillary tangles (NFT) are considered the two hallmarks of AD pathology. Proteolytic cleavage of the amyloid precursor protein (APP) by both beta- and gamma-secretases generates a 40 or 42 amino acid A $\beta$  peptide (Figure 1.1) (Masters & Selkoe, 2012; Pruta *et al.*, 2013). AD is also considered a tauopathy (Hernández & Avila, 2007). Tau protein, normally present in neurons, binds microtubules (MT) and promotes assembly to stabilize MTs

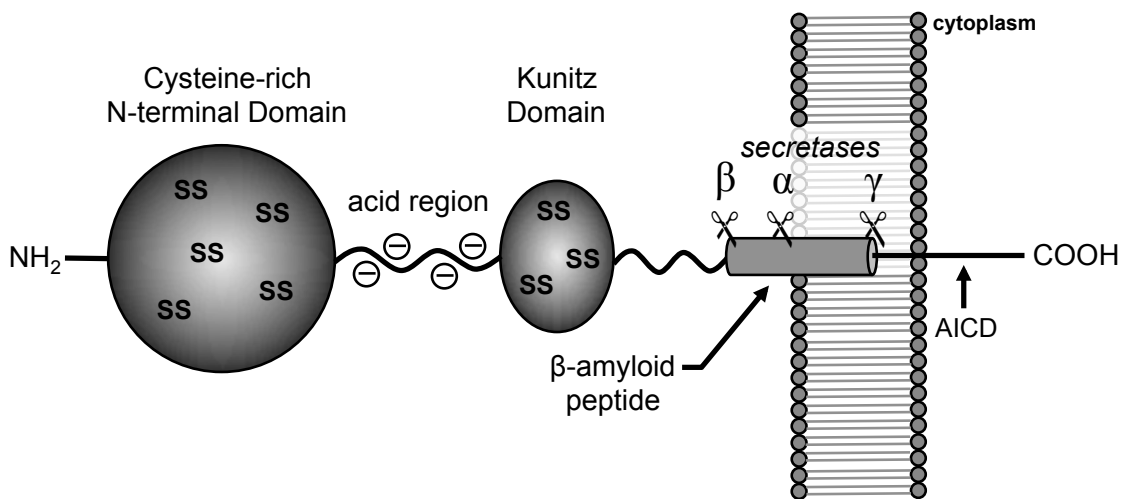


Figure 1.1: APP proteolytic processing. APP cleavage by  $\alpha$ -secretase releases the soluble N-terminal fragment and leaves a membrane-inserted fragment in the non-amyloidogenic pathway. Subsequent cleavage by  $\gamma$ -secretase releases the APP intracellular domain (AICD). Alternatively, APP cleavage first by  $\beta$ - and then by  $\gamma$ -secretase produces the amyloidogenic  $A\beta_{1-42}$  peptide.

and promote vesicle transport (Figure 1.2). Phosphorylation of tau in its microtubule-binding domain prevents its binding to MT. Tau released from MTs undergoes additional phosphorylation (hyperphosphorylation) that permits its assembly into paired helical filaments that aggregate and play a role in synaptic loss (Thies and Mendelkowitz, 2007). Paired helical filaments are components of neuropil threads in neurites that may also accumulate in cell bodies as neurofibrillary tangles (NFT) (Hernández & Avila, 2007). Repetitive mTBI also results in enhanced NFT formation, demonstrating a relationship between the pathogenesis of neuroinflammatory disorders and neurodegenerative diseases (Yoshiyama *et al.*, 2005). Though AD is defined pathologically by plaques and tangles, they do not necessarily correlate with cognitive status (Hernández & Avila, 2007; Scheff *et al.*, 2014).

### **ADF/Cofilin-Actin Rod Formation**

Specific oligomers of A $\beta$  will initiate the dynamic remodeling of actin into rod-like neuritic occlusions (Minamide *et al.*, 2000; Davis *et al.*, 2009). Dynamic processes that regulate actin and microtubule networks dictate cellular movement and morphology. Actin exists in both unassembled (G-actin) and filamentous (F-actin) forms. G-actin will spontaneously assemble to form F-actin *in vitro* under physiological ionic conditions in a process that is tightly regulated by monomer sequestering proteins (Sun *et al.*, 1995) and capping proteins (Cooper & Schafer, 2000; Sarmiere & Bamberg, 2003). One such process involves actin-depolymerizing factor (ADF)/cofilin, a family of proteins that enhances the severing and turnover of actin filaments by binding cooperatively to ADP-actin thereby replenishing a pool of free actin monomers and enhancing dynamic

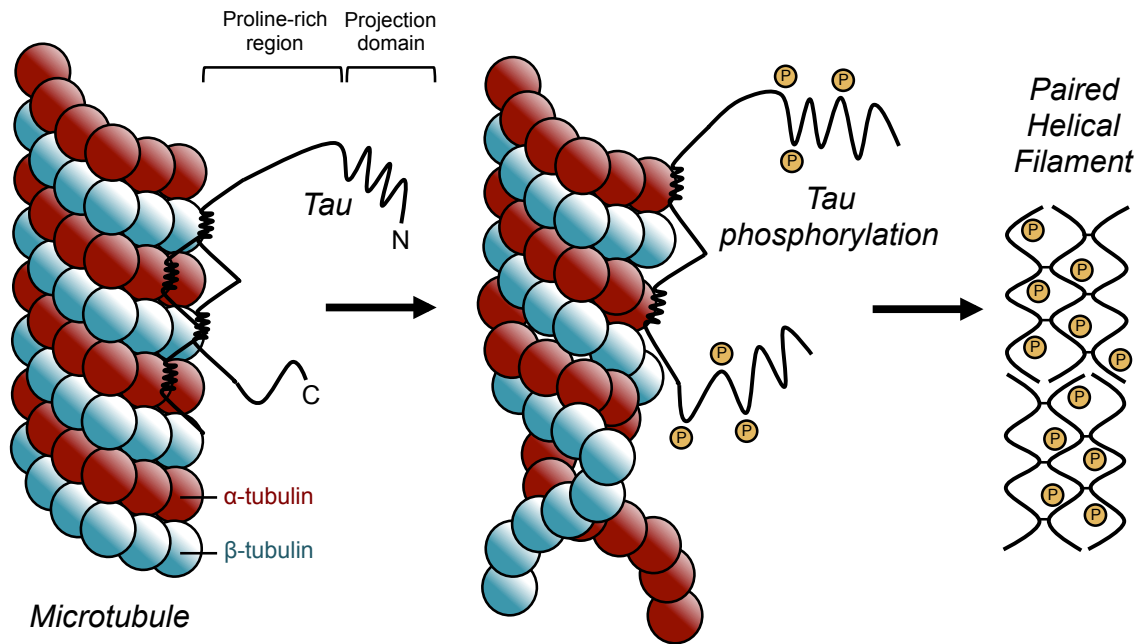


Figure 1.2: Tau hyperphosphorylation and microtubule destabilization. Tau protein is a highly soluble microtubule-associated protein (MAP) found predominantly but not exclusively in neurons. Tau proteins contain a distinct microtubule-binding domain, whereas a proline-rich domain has been shown to sequester G-actin. In contrast, the N-terminal projection domain is involved with microtubule spacing. Phosphorylation of tau in the MT binding domain releases it from microtubules, and permits assembly of hyperphosphorylated tau into paired helical filaments that deposit as neuropil threads or aggregate further into neurofibrillary tangles (NFT). Along with amyloid plaques, NFTs are a pathological hallmark of Alzheimer disease.

turnover (Figure 1.3) (Andrianantoandro & Pollard, 2006).

Activation of cofilin requires its dephosphorylation by protein phosphatases, the most specific ones being Slingshot (SSH) or Chronophin (CIN) (Niwa *et al.*, 2002; Huang *et al.* 2006). Once activated, if reactive oxygen species (ROS) are above some threshold, the sulfhydryl oxidation of cofilin's four cysteine residues may occur in different ways. The formation of two intramolecular disulfide bonds eliminates cofilin's ability to bind actin and instead targets cofilin to mitochondria where it mediates apoptosis via cytochrome *c* release (Klamt *et al.*, 2009; Schönhofen *et al.*, 2014). A $\beta$ -induced neuronal apoptosis requires the scaffolding protein RanBP9, a mediator of cofilin activation and ROS production (Roh *et al.*, 2013). Conversely, cofilin in which sulfhydryl oxidation forms one intermolecular disulfide (Bernstein *et al.*, 2012) is incorporated into rod-like actin bundles (rods) that may occlude neurites, inhibiting vesicular transport that is necessary for synaptic function (Figure 1.4) (Minamide *et al.*, 2000; Maloney *et al.*, 2005; Cichon *et al.*, 2012). Specifically, cofilin-actin rods result in a global loss of trafficking of APP-containing vesicles (Mi *et al.*, 2013) that are normally trafficked anterogradely to the plasma membrane and retrogradely for lysosomal degradation (Ehehalt *et al.*, 2003; Thinakaran & Koo, 2008). Rods may also mediate synaptic loss by sequestering cofilin from dendritic spines where it functions in long-term potentiation (LTP) (Gu *et al.*, 2010; Schönhofen P *et al.*, 2014). Although rods block transport and cause synaptic dysfunction, they also spare ATP used in actin turnover (Bernstein *et al.*, 2006) and may promote neuronal survival by preventing complete cofilin oxidation and thus its mitochondrial targeting.

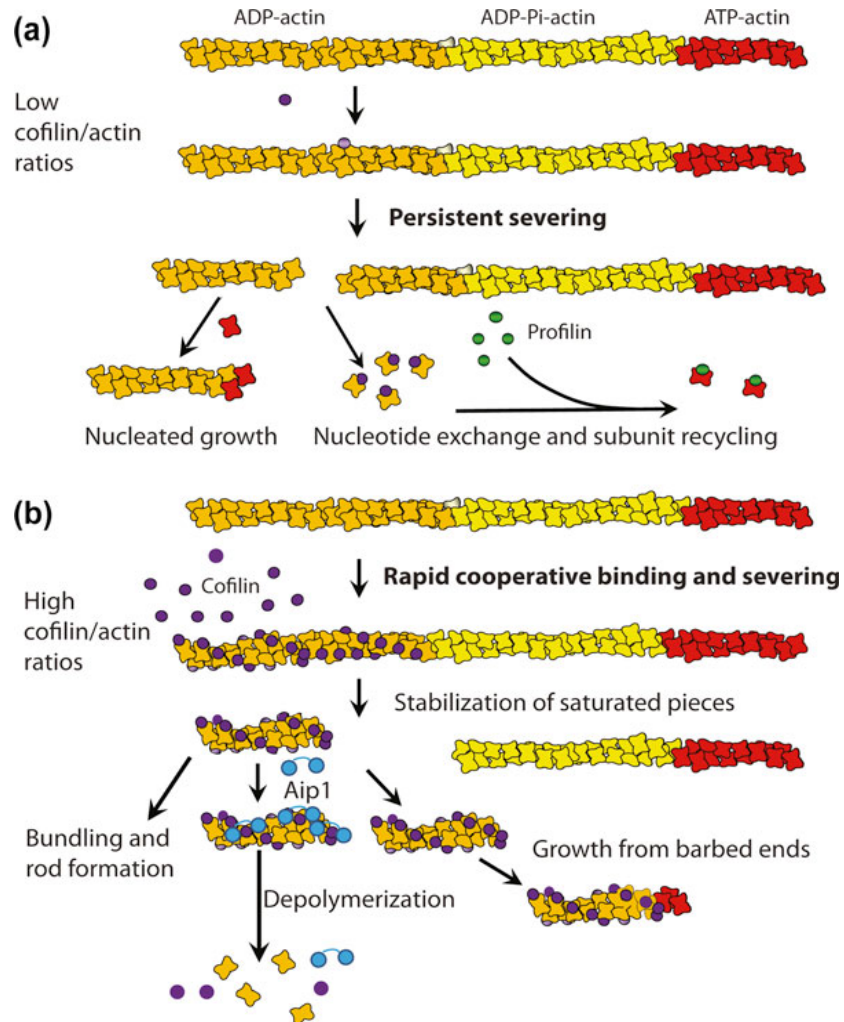


Figure 1.3: ADF/cofilin regulates actin dynamics. (A) At steady-state and low molar ratios of ADF/cofilin:actin, a family of actin-severing proteins, actin filaments (F-actin) undergo treadmilling. ATP-bound actin is added to the plus end of a growing filament followed by the hydrolysis of the  $\gamma$ -phosphate and release of inorganic phosphate ( $P_i$ ). ADP-actin stabilizes a twisted conformation that allows for increased depolymerization from the minus end. G-actin monomers undergo nucleotide exchange, removal of ADP and addition of ATP, enhanced by profilin. (B) At high ADF/cofilin:actin ratios, cofilin can initiate the bundling of actin filaments into 1:1 cofilin:actin rods (Fig. 1 in Bamberg & Bernstein, 2010).

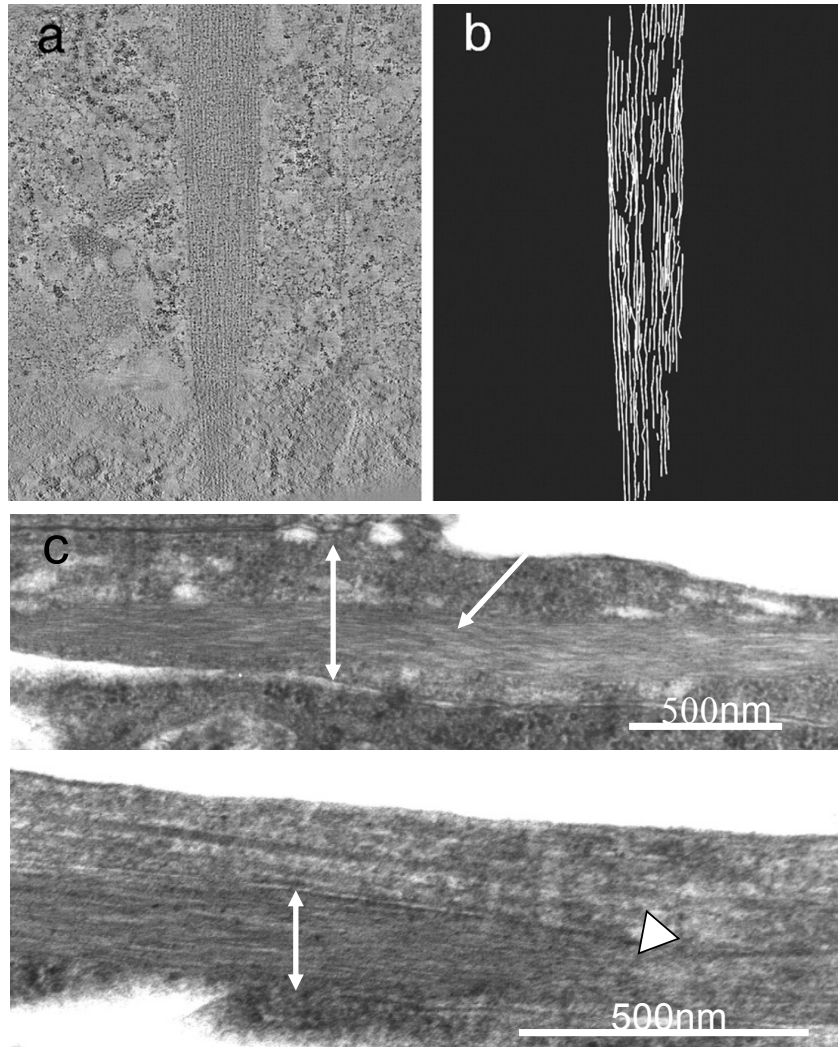


Figure 1.4: Cofilin-actin rods occlude the entire neurite, obstructing vesicular transport. Bundles of ADF/cofilin-saturated actin filaments (rods). (A-B) Tracing individual filaments using tomographic analysis reveals the tapered end of a rod formed in an ATP depleted A4.8 cell expressing *Xenopus* ADF/cofilin (XAC)-GFP (Minamide *et al.*, 2010). (C) Rods grow to occlude the entire neurite, blocking vesicular transport (white spheres) between two neurons (Minamide *et al.*, 2000).

The hippocampus, a region associated with learning and memory, is a primary site where neurodegenerative effects can be seen in cognitive impairment (Braak & Braak, 1995). Rod formation occurs in stimuli-specific hippocampal populations in response to distinct sources of oxidative stress and inflammation (Davis *et al.*, 2009; Bamburg *et al.*, 2010). However, most rod activity can be linked by source of stimuli to circuitry between the dentate gyrus (DG) and cornu ammonis (CA1-4 subdivisions) in the rodent hippocampus (Figure 1.5). A $\beta$ -induced rods have a robust preference for the DG, whereas rods formed in response to glutamate are most prevalent in the CA1/3 regions (Davis *et al.*, 2009). Each of the aforementioned stressors leads to synaptic loss identified in AD. Additionally, markers for synaptic loss were found in the DG of an individual with progressive dementia but without plaques or tangles (Hamos *et al.*, 1989). If rods indeed mediate synaptic loss associated with AD and other neurodegenerative diseases, they may represent a potential target for therapeutic intervention.

The accumulation of rods is likely to cause synaptic loss without neuronal loss, a process that occurs early in dementias. Rods are observed in brains from human AD subjects and may represent a common mechanism for synaptic loss that underlies other neurodegenerative diseases (Minamide *et al.*, 2000). Sporadic AD is poorly understood, but has many epigenetic causes and occurs in about 50% of those reaching the age of 85 (Alzheimer Association, 2014). Familial AD, which accounts for less than 5% of all cases (Bertram & Tanzi, 2004), occurs as a result of genetic mutations that lead to enhanced A $\beta$  production from APP or its reduced clearance (Maloney & Bamburg, 2006; Bagyinszky *et al.*, 2014).

Several recent studies related to APP suggest that A $\beta$  plays a significant role in

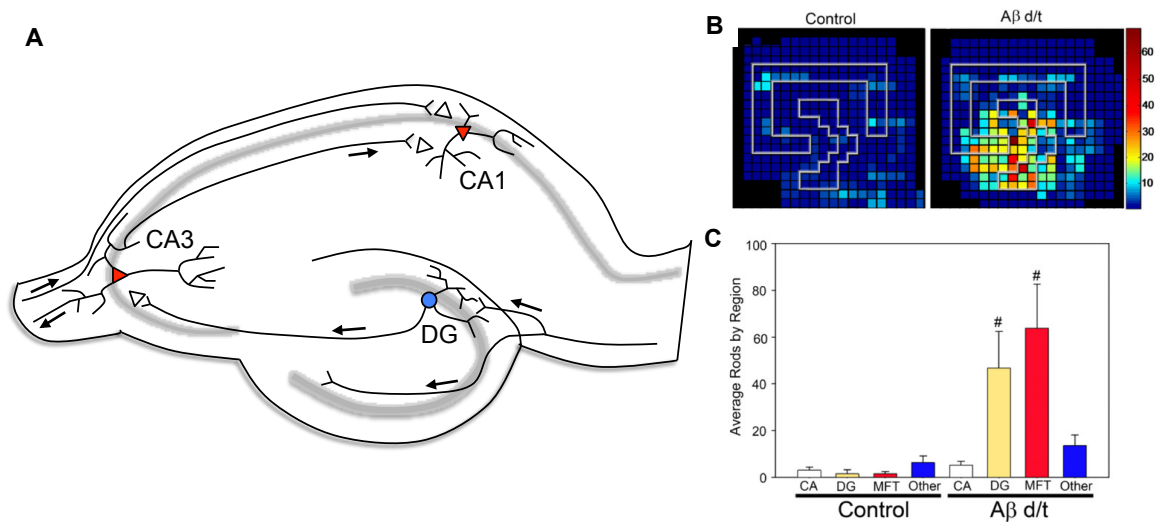


Figure 1.5: Circuitry of the hippocampus: dentate gyrus and cornu ammonis. (A) Diagram of the hippocampus showing circuitry between the distinct regions of the dentate gyrus (DG) and cornu ammonis (CA, subdivisions 1-3). (B-C) Rod formation occurs in stimuli-specific hippocampal populations in response to distinct sources of oxidative stress. Specifically, rod activity can be linked by source of stimuli to circuitry between the DG and CA. A $\beta$ -induced rods have a robust preference for the DG whereas rods formed in response to glutamate (data not shown) accumulate mainly in the CA1/3 regions (Davis *et al.*, 2009; 2011).

the development of cognitive deficiencies associated with aging and Alzheimer disease (Jonsson *et al.*, 2012; Pluta *et al.*, 2013). Levels of A $\beta$  extracted from the frontal cortex of AD subjects vary widely (McDonald *et al.*, 2012) and amyloid profiles overlap considerably with subjects of similar age classified as cognitively normal (Moore *et al.*, 2012). This implies that cognitive decline is not simply due to the amount of A $\beta$  produced, but also to its post-production modification and/or assembly into oligomers (Masters & Selkoe, 2012). Sodium dodecyl sulfate (SDS)-stable dimers are a major form of soluble A $\beta$  extracted from AD brains, but do not correlate with increased plaque pathology (McDonald *et al.*, 2010, 2012). Small SDS-stable A $\beta$  oligomers can be formed by an *in vitro* oxidation of synthetic human A $\beta$ <sub>1-42</sub> under physiologically relevant conditions (Atwood *et al.*, 2004), which increases its rod-inducing activity by 600 fold (Davis *et al.*, 2011). This activity is still less potent than that obtained with SDS-stable dimer/trimers (A $\beta$ d/t) fractionated from culture medium of a line (7PA2) of Chinese hamster ovary (CHO) cells made to secrete human A $\beta$  (Cleary *et al.*, 2005). However, together these findings suggest that enhanced oxidative stress may play a role in making A $\beta$  more effective in synapse elimination through rod formation.

### **Proposal For Two Independent Pathways for Rod Formation**

Neurodegenerative stimuli that activate cofilin include ATP-depletion, excitotoxic glutamate (Minamide *et al.*, 2000), and soluble beta-amyloid (A $\beta$ ) peptides (Maloney *et al.*, 2005; Davis *et al.*, 2009). Mitochondrial inhibitors such as antimycin A (Whiteman *et al.*, 2009) and excitotoxic levels of glutamate induce rods within minutes, whereas A $\beta$

mediated rod induction is a much slower process in a class that is the focus of the experiments described in this thesis.

The aims of this thesis are to further distinguish the pathways for rapid and slow rod formation. We demonstrate that slow rod formation by A $\beta$ d/t and proinflammatory cytokines depends on the presence of PrP<sup>C</sup>, and we further characterize the PrP<sup>C</sup>-dependent signaling pathway for cofilin-actin rod formation (Figure 1.6). We show here that various proinflammatory cytokines and A $\beta$ d/t target an identical population of hippocampal neurons for the prion-dependent activation of NADPH oxidase (NOX) to generate ROS (Walsh *et al.*, 2014). We also show that perturbing ROS generation of existing rod structures leads to their rapid dissolution, suggesting that a minimal cytokine- or amyloid-mediated ROS threshold must be exceeded in order to sustain rod formation.

Using the naturally occurring plant pentacyclic triterpene, ursolic acid (UA), and various pharmacological inhibitors, we illustrate that this mechanism for slow rod formation is reversible and may involve a coalescence of PrP<sup>C</sup>-containing membrane microdomains. We support this idea here by demonstrating that overexpression of PrP<sup>C</sup> without an external stimulus is sufficient to induce rods. Taken together, synaptic loss through PrP<sup>C</sup>-dependent signaling may be explained by the initial formation of cofilin-actin rods, and may present an underlying mechanism for the onset of many neurodegenerative disorders.

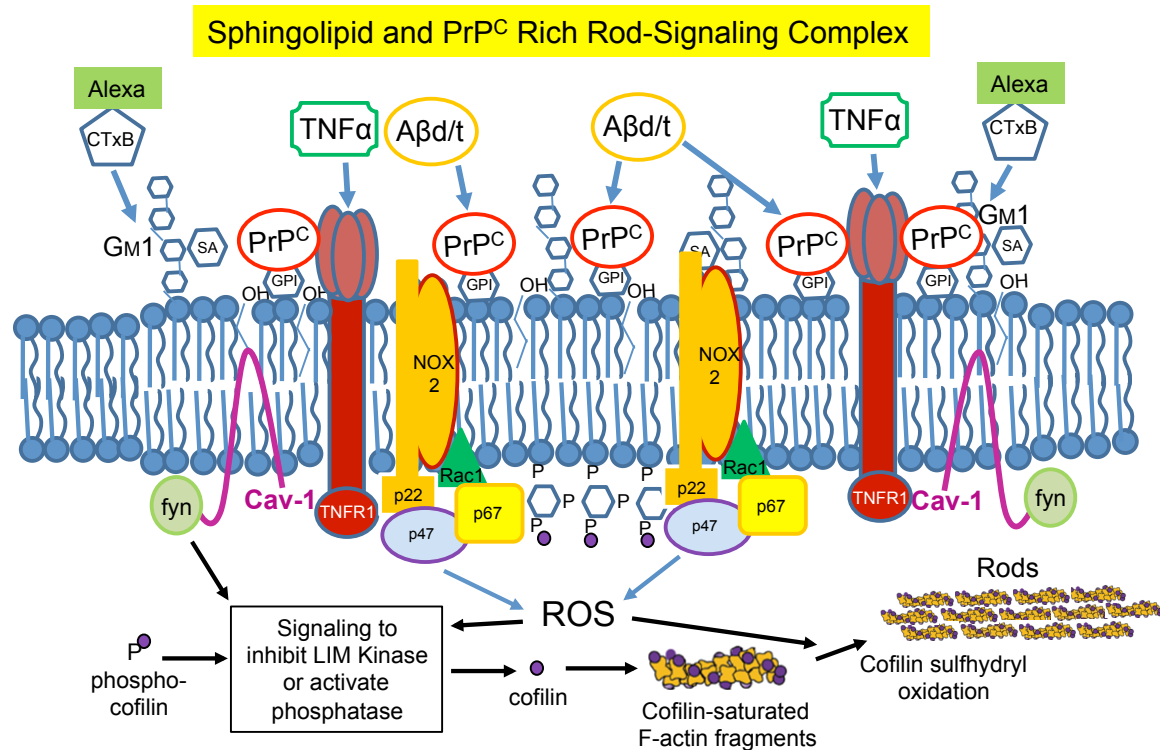


Figure 1.6: Schematic hypothetical model of a prion-mediated signaling mechanism for rod formation. A proposed model linking oxidative stressors A $\beta$ d/t and TNF $\alpha$  to cofilin-actin rod formation has been constructed based upon live-cell visualization of some of its components. Overexpression of PrP<sup>C</sup> alone is sufficient to induce rods in a NOX-dependent manner, suggesting enlargement of membrane signaling domains in which resultant ROS generation exceeds a rod-inducing threshold. This inducible oxidizing environment both maintains dephosphorylation-dependent activation of cofilin and initiates intramolecular disulfide bond formation in dephosphorylated cofilin to permit bundling of cofilin-saturated filaments. The dynamics of rod dissolution and reversal upon addition of several NOX inhibitors further suggests that loss of contributing components to the membrane complex may generate levels of ROS that fail to reach this threshold for rod maintenance.

CHAPTER 2:  
PROINFLAMMATORY CYTOKINES AND  $\beta$ -AMYLOID INDUCE COFILIN-ACTIN ROD  
FORMATION

**Introduction**

Cofilin-actin rods form from minutes to hours in neurons stressed with various oxidizing agents (Minamide *et al.*, 2000; Maloney *et al.*, 2005; Davis *et al.*, 2009; Whiteman *et al.*, 2009). When fluorescently tagged wild type (wt) cofilin is used to image rods in living cells, its overexpression alone induces spontaneous rod formation, which is exacerbated by the photostress of microscopy (Bernstein *et al.*, 2006; Chichon *et al.*, 2012; Mi *et al.*, 2013). Rods formed under these conditions undermine the interpretation of experiments addressing the roles of rod formation and reversibility in response to physiologically relevant stimuli. Therefore, surface residue mutants of cofilin were characterized to identify a mutant that did not form rods when simply overexpressed in cells but was still incorporated into rods formed by endogenous cofilin in cells stressed with an external stimulus (Mi *et al.*, 2013). One of the mutants, cofilinR21Q fused to mRFP, did not form spontaneous rods even when expressed at levels 3-5 fold over endogenous cofilin. This mutant incorporated into all rods that formed rapidly in neurons in response to excitotoxic glutamate, but was incorporated into only about half of the rods that formed slowly in response to A $\beta$  and TNF $\alpha$ . This suggests that its weaker actin binding allows it to be excluded from slower forming rods; nevertheless, it can be used as a genetically encoded indicator for studying rod dynamics in neurons (Figure 2.1). Here we show that the cofilinR21Q-mRFP adenovirus can be used for live cell imaging.

Proinflammatory cytokines, such as tumor necrosis factor-alpha (TNF $\alpha$ ) and interleukins (IL)-1 $\beta$  and IL-6, initiate and enhance the oxidative cascade of neurodegeneration (Mrek & Griffin, 2005; Griffin & Barger, 2010). These cytokines are rapidly produced in response to infectious agents (HIV and malaria) (Feuerstein *et al.*, 1994) and in various types of neuroinflammatory traumatic brain injury (TBI) (Lin & Wen, 2013). However, the mechanism(s) by which proinflammatory cytokines contribute to circuitry abnormalities via synaptic dysfunction is not well understood. We show here that rods are induced by proinflammatory cytokines and A $\beta$  in the identical subpopulation of hippocampal neurons.

TNF $\alpha$  and other proinflammatory cytokines increase cofilin phosphorylation within 4 h in endothelial cells through a RhoA/Rho kinase-dependent pathway (Campos *et al.*, 2009). Conversely, cofilin dephosphorylation was observed in neurons treated with fast rod-inducing agents, such as glutamate, ATP-depletion and peroxide treatments (Schönhoffen *et al.*, 2014). Previously, we have demonstrated that dephosphorylated cofilin was the predominant form of cofilin present along neurites of neurons containing A $\beta$ -induced rods (Maloney *et al.*, 2005). Here we show that treatment with TNF $\alpha$  initiates an increase in cofilin dephosphorylation in neurites containing rods, which is also highest directly over the rod, but which increases over time outside of the rod region.

## **Materials and Methods**

*Reagents.* Unless stated otherwise all chemical reagents are from Sigma-Aldrich Co. (St. Louis, MO), and all tissue culture and fluorescence reagents are from Life

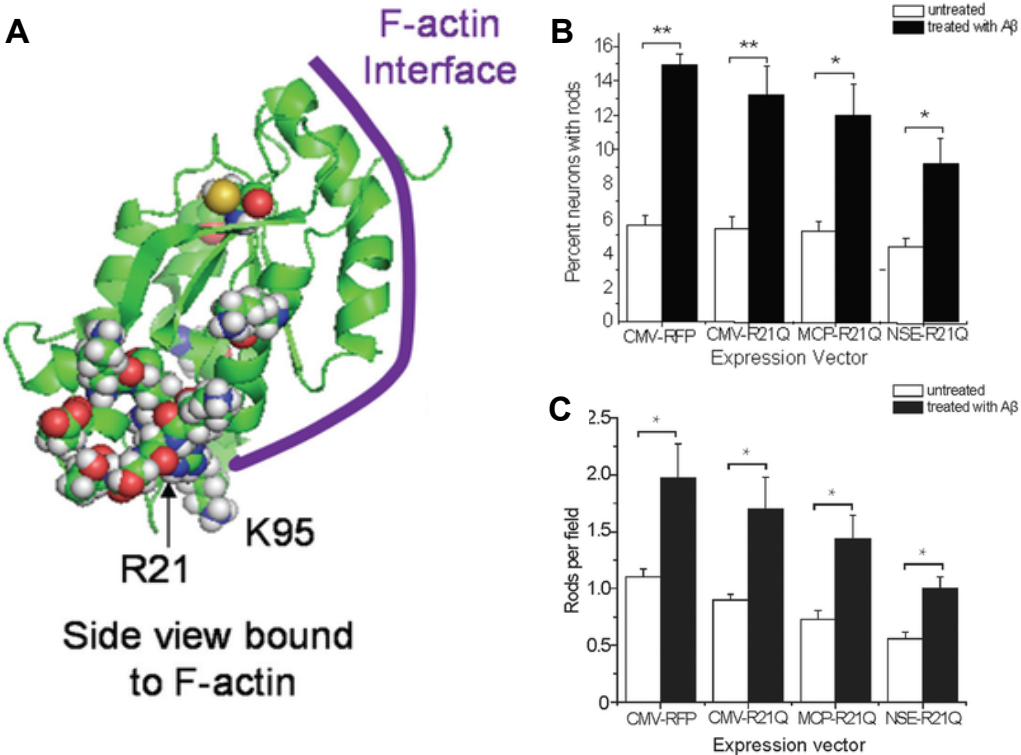


Figure 2.1: CofilinR21Q-mRFP is a genetically encoded rod reporter. Cofilin overexpression using a wild-type (wt)-cofilin-mRFP adenovirus generates spontaneous rod formation, which is exacerbated by the photo-stress of microscopy. Therefore Mi *et al.* (2013) generated various cofilin mutants that will incorporate into rods formed from endogenous cofilin but do not induce rods when overexpressed. (A) Side view of a PyMOL model for cofilin showing the approximate F-actin binding interface. One such mutant, R21Q, was identified to have about a 10-fold weaker interaction with F-actin than wt-cofilin, yet is still incorporated into induced rods (Mi *et al.*, 2013). Rods formed after treatment with A $\beta$ /t are 2-3 fold higher than untreated neurons regardless of which promoter drives cofilinR21Q-mRFP expression as examined either by analysis of the (B) percent of neurons containing rods or (C) approximate rods per cell body (Mi *et al.*, 2013).

Technologies (Invitrogen Corp., Carlsbad, CA).

*Neuronal Cell Culture.* Rat E18 cortical and hippocampal neurons were obtained from time-pregnant dams (Harlan, Indianapolis, IN) and used fresh or stored frozen (Minamide *et al.*, 2000). Cells (15-20,000) were plated on poly-D-lysine-coated coverslips (Glaswarenfabrik Karl Hecht KG, Sondheim, Germany) either in drilled out 35 mm tissue culture dishes (25,000 cells per 22 mm square coverslips attached with aquarium sealant) (All-glass Aquarium) or in 24 well plates (15-20,000 cells per 15 mm round coverslips). Cells were cultured in Neurobasal SFM (serum-free medium) (GIBCO, Grand Island, NY), supplemented with B27 (used at 1X; Life Technologies), GlutaMax (25  $\mu$ l/10 ml; Life Technologies) and Penicillin/Streptomycin (50 units/ml/50  $\mu$ g/ml final concentration). Cultures were maintained in a 5% CO<sub>2</sub> incubator at 37°C and SFM was replaced every 2-3 days.

*Adenovirus Production.* Adenovirus for cofilinR21Q-mRFP mutant was made, amplified, and titered using the AdEasy system (Mi *et al.*, 2013). For adenovirus production, vectors were linearized, electroporated into BJ5183 *E. coli* containing the AdEasy virus DNA, bacteria containing homologous recombinants within the AdEasy DNA were selected, viral DNAs containing the different promoter driven cofilin constructs were isolated, linearized, and transfected into HEK293 cells, and the produced virus amplified twice more and titered (Minamide *et al.*, 2003).

*Amyloid Beta Peptide Preparation.* A $\beta$ d/t was obtained from culture medium of 7PA2 Chinese hamster ovary cells expressing an AD-mutant, human APP (Podlisny *et al.*, 1995). Following a 16-hour serum-starvation, the 10 ml of culture medium was removed and centrifuged (Eppendorf 5810R) at 1000 rpm for 10 minutes at 4°C.

Supernatant was then filter-concentrated (Amicon Ultracel 3K centrifugal filters) from 10 ml to ~1 ml, which is used for A $\beta$  purification, or quick-frozen and stored (-80°C) for later use. About 1 ml of concentrated medium was then injected onto a FPLC Superdex 75 (#5) resin column in a volatile ammonium acetate buffer (Cleary *et al.*, 2005) and fractions were collected in Millipore 15 ml conical tubes. Replicate sample runs of 1 ml loads allowed collection in the same tubes for up to 7 or 8 repeats per day (column profiles monitored by UV absorbance were identical between runs). Fractions identified as containing A $\beta$ d/t (see western blotting below) were pooled and considered to contain all the A $\beta$ d/t from the starting volume of medium. These were freeze-dried in aliquots that allowed them to be resolubilized in Neurobasal medium for direct addition to neuronal cultures. A volume of 200  $\mu$ l was removed from a range of fractions in 15 ml conical tubes for running on gels to identify which fractions contained dimer/trimer, and stored at -20°C.

*Western blotting.* Aliquots (200  $\mu$ l) of each fraction were freeze-dried and then solubilized in SDS buffer for electrophoresis on a 10-20% acrylamide gradient pre-cast Mini-PROTEAN gel (Bio-Rad, Hercules, CA). Proteins were transferred onto nitrocellulose (0.1  $\mu$ m; Whatman, Dassel, Germany) by electroblotting 2 h at 300 mA in Western transfer buffer (0.3% Tris, 1.4% glycine, 20% methanol), the membrane was heated to boiling for 10 min in phosphate buffered saline (PBS), blocked at room temperature in 1% bovine serum albumin (BSA)/Tris-buffered saline (TBS) for 30 min, and incubated overnight at 4°C in primary antibody, A $\beta$  monoclonal 6E10 (Covance, Dedham, MA; 1:1000 in TBS plus 0.05% Tween-20 (TBST)). Blots were incubated in secondary antibodies (DyLight 680 or 800 conjugates, 1:15,000; Thermo Scientific,

Rockford, IL) for 45 min at room temperature. Blots were washed in TBST 10 times over the course of an hour, and imaged with a LI-COR Odyssey Infrared Imaging System. Fractions containing dimer/trimer (12 & 13) were pooled and then aliquoted for freeze drying in 1.5 ml, 3 ml, 4.5 ml, 6 ml, or 9 ml fractions to be used in culture.

#### *Cytokine Preparation.*

TNF $\alpha$ : TNF $\alpha$  (Enzo Life Sciences) was dissolved in sterile Neurobasal medium containing 0.1% BSA, quick frozen at 20  $\mu$ g/ml (400X final concentration) in liquid N<sub>2</sub> in 10  $\mu$ l aliquots, and stored at -80°C. It was used for treatment at a final concentration of 50 ng/ml (2.87 nM) (concentration based on dose-response rod induction, Figure 2.3A). TNF $\alpha$  treatments varied from 12-24 hour, but proved to be toxic to neuronal cultures after 24 hours (time of treatment based on time course rod induction, Figure 2.3B). Cell cultures with a medium change prior to the day of fixation served as controls.

IL-1 $\beta$ /6: IL-1 $\beta$  and IL-6 (PeproTech, Inc., Rocky Hill, NJ) were dissolved in Neurobasal medium with 0.1% BSA, quick-frozen at 5  $\mu$ g/ml in 20  $\mu$ l aliquots, and stored -80°C. Both cytokines were used at 50 ng/ml, the same concentration as TNF $\alpha$ .

#### *Cell Treatments*

Adenovirus infection. Relative expression levels driven by different promoters were determined by infecting SAOS2 cells, HeLa cells, and N2a neuroblastoma cells with adenoviruses at 25-50 multiplicity of infection (MOI) and preparing cell extracts for immunoblot analysis at 48-72 h post-infection (Mi *et al.*, 2013). Relative intensities of bands corresponding to cofilin-mRFP (47 kDa) to endogenous cofilin (19 kDa) were quantified to determine strength of expression. In N2a cells in which all promoters are active the ratio was ~5X for the human cytomegalovirus (CMV) promoter, ~2X for the

mouse cofilin promoter, and ~1.5X for the neuron-specific enolase (NSE) promoter (Mi *et al.*, 2013). The adenovirus for cofilinR21Q-mRFP expression driven by the CMV promoter was used in subsequent infections for E18 rat hippocampal neuronal cultures. Cells were maintained in a 5% CO<sub>2</sub> incubator at 37°C for 3 days before medium change and infection at 150 MOI for 40 h.

Rod inducing treatments. Neurons were treated with A $\beta$ d/t by reconstituting freeze-dried aliquots in Neurobasal medium to their fractionated volumes, considered as 1X (approximately 250 pM, estimated by immunoblotting against synthetic human A $\beta$ <sub>1-42</sub> (Davis *et al.*, 2011)). Cell cultures with a medium change prior to the day of fixation served as controls.

*Fixation and Immunolabelling.* For rod quantification, cells were fixed in 4% formaldehyde, 0.1% glutaraldehyde in PBS for 45 min at room temperature, permeabilized with methanol (chill to -20°C) for 3 min, and blocked with 5% goat serum in 1% BSA/TBS before immunolabeling with affinity purified rabbit 1439 antibody (2 ng/ $\mu$ l) (Shaw *et al.*, 2004) and fluorescent secondary antibodies. Coverslips were mounted with ProLong Gold Antifade (Invitrogen). For ratio imaging of phosphoADF/cofilin versus total cofilin, rabbit 4321 phosphoADF/cofilin antibody (affinity purified at 1 ng/ $\mu$ l) and MAb22 (Abe *et al.*, 1989) (total IgG at 2 ng/ $\mu$ l) against total cofilin were used as primary antibodies. Secondary goat anti-rabbit (1:450) and donkey anti-mouse antibodies (1:1000) were labeled with Alexa(s) 488, 594 or 648 (Invitrogen).

*Imaging and Analysis.* Fluorescence microscopy was performed on a Nikon Diaphot epifluorescence microscope using a 60X (1.40 numerical aperture) oil objective. Images were captured with CoolSnap ES camera driven by Metamorph software

(Molecular Devices, Downingtown, PA). Ratiometric analysis to quantify TNF $\alpha$ -induced cofilin dephosphorylation was performed using Metamorph. Experimental quantification consisted of scoring 100 random cells in triplicate samples to determine the number of cells that contained rods. Rod-containing neurons interacting with other neurons were scored as one positive neuron since it was not possible to determine from which soma a rod containing process originated, whereas non-rod-containing neuronal networks were scored for each soma that they contained since none of the neurons within the network had rods. All scoring was done blindly, and experiments were repeated independently at least three times, giving between 800 and 1200 neurons scored for each treatment.

Live cell imaging was performed on a Nikon Eclipse 2000 inverted total internal reflection fluorescence (TIRF) microscope with 405, 488, 561 and 640 nm laser lines, perfect focus control, XY piezo Z stage, CO<sub>2</sub>-controlled stage incubator, 100X (1.48 NA), 60X (1.40 NA) and 40X (0.75 NA) objectives and Andor iXon3 EMCCD camera. Images were captured and analyzed using Nikon Elements software.

*Statistics.* All experiments were run with at least triplicate samples and were repeated at least three times. For all figures derived from the results explained here, statistical significance between samples with one variable was calculated using Student's "*t*" test, whereas significance of differences between groups with multiple variables was performed by ANOVA with Tukey's post-hoc analysis using JMP software (SAS Institute Inc.) Statistical comparisons in the figures utilize the following symbols for the p values given, unless noted otherwise: \* p<0.01, \*\* p<0.05, # p<0.001, ## p<0.005, NS = non-significance.

## Results

*CofilinR21Q-mRFP functions as a rod reporter for real time imaging.* In live neurons, the study of cofilin-actin rod formation induced by a specific external stimuli (i.e. A $\beta$ ) has been limited because overexpression of fluorescently-tagged wt cofilin results in formation of abundant “spontaneous” rods which are exacerbated by the photostress of imaging (Bernstein *et al.*, 2006; Cichon *et al.*, 2012). To demonstrate that cofilinR21Q-mRFP can be used to study rod dynamics in real time, we compared rod formation in neurons expressing cofilin-wt-mRFP with neurons expressing cofilinR21Q-mRFP during 2 h of imaging. Only neurons expressing cofilin-wt-mRFP formed spontaneous rods (Figure 2.2).

*Proinflammatory cytokines induce cofilin-actin rods.* Proinflammatory cytokines orchestrate the generation of ROS in neurons (Barth *et al.*, 2009), and cofilin oxidation is a prerequisite for the formation of cofilin-actin rods (Bernstein *et al.*, 2012). Thus, we examined whether the prominent cytokines associated with neuroinflammation (TNF $\alpha$ , IL-1 $\beta$ , IL-6) elicit rod formation in dissociated rat (E18) hippocampal neurons. Each of the three cytokines at 5 ng/ml induced rods significantly ( $p < 0.05$ ) above untreated control, and at 50-100 ng/ml induced rods in a maximum of 17-26% of the neurons ( $p < 0.005$ ) (Figure 2.3A). The time course of rod formation mediated by 50 ng/ml TNF $\alpha$  was comparable to that of the optimal concentration of SDS-stable A $\beta$ d/t (~250 pM), reaching a significant difference ( $p < 0.01$ ) over controls by 4 h with 50% maximal response reached by 6 h of treatment (Figure 2.3B). Two time point analyses of neurons treated with IL-1 $\beta$  and IL-6 showed identical behavior to TNF $\alpha$ .

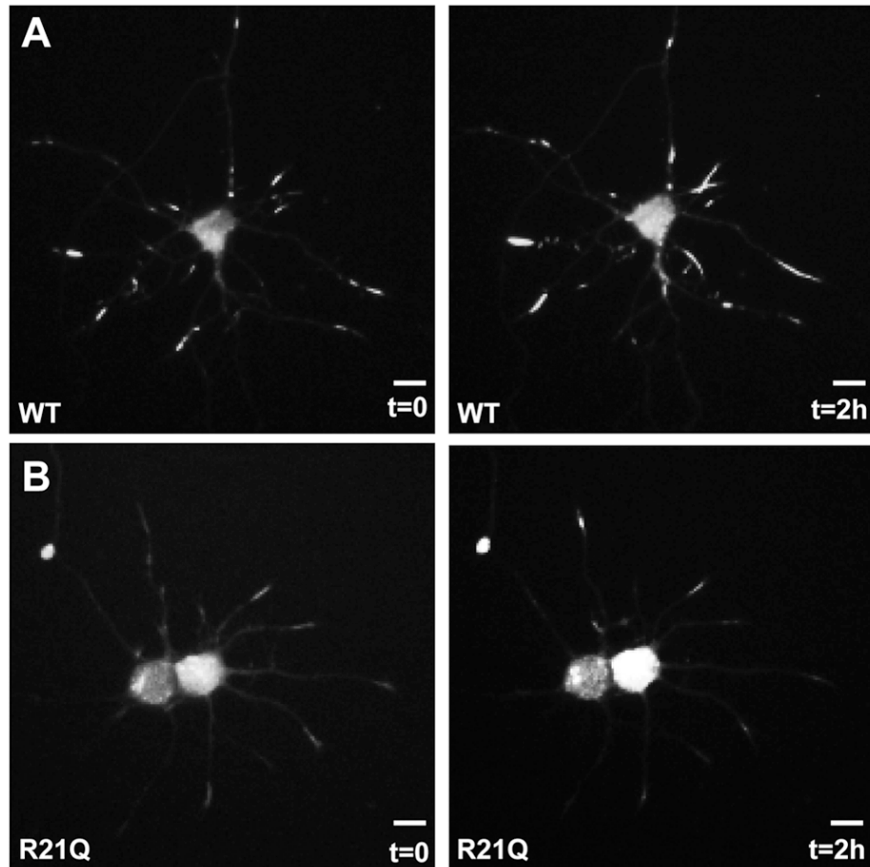


Figure 2.2: CofilinR21Q-mRFP rods in live cell imaging: Data in part with Mi *et al.* finding that the R21Q cofilin mutant serves as a rod reporter in live cell imaging. (A) Spontaneous rods form as a result of 2 h TIRF microscopy imaging. (B) CofilinR21Q-mRFP does not form spontaneous rods as a result of imaging, thus was used in all subsequent live cell experiments for rod formation.

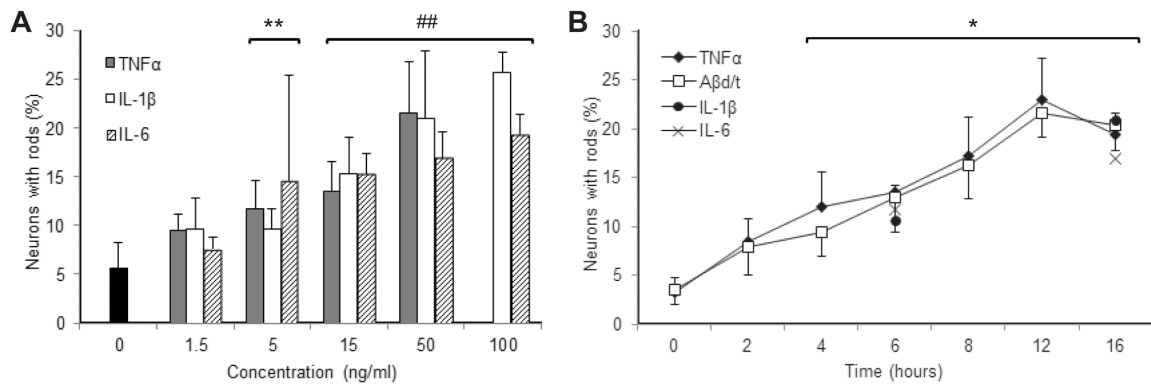


Figure 2.3: Proinflammatory cytokines dose-response curves and time course of rod formation in dissociated hippocampal neurons. (A) Percent of neurons with rods at 20 h after treatment with TNF $\alpha$ , IL-1 $\beta$  and IL-6 show a similar dose-response. The maximum response level of approximately 20% of the neurons was reached at ~50 ng/ml for each cytokine, thus this concentration was selected for further studies. (B) The time course of rod formation in dissociated hippocampal neurons treated with 50 ng/ml TNF $\alpha$  is remarkably similar to that for A $\beta$ d/t (~250 pM). Six and 16 h time points were performed with IL-1 $\beta$  and IL-6 and they are not significantly different from TNF $\alpha$  and A $\beta$ d/t responses at the same times. Significant values with respect to untreated or zero time controls \*(p<0.01), \*\*(p<0.05), ###(p<0.005). Error bars in this and all subsequent figures are standard deviations.

*TNF $\alpha$  and A $\beta$ d/t target the same population of hippocampal neurons.* Since A $\beta$  and TNF $\alpha$  shared similar kinetics of rod formation and affected the same maximum number of neurons, we suspected that an identical population of hippocampal neurons was sensitive to either treatment. To test this, we treated cultures of dissociated neurons with optimal rod-inducing concentrations of A $\beta$ d/t (~250 pM) or TNF $\alpha$  (2.9 nM, 50 ng/ml) alone and combined. After 24 h of treatment, neurons were fixed, immunostained for ADF/cofilin, and rods quantified both in terms of the percent of neurons with rods and the number of rods per soma the (number rod index), which gives an estimate of the robustness of a rod response for each neuron responding to a treatment. A $\beta$ d/t and TNF $\alpha$  induce rods in 20-25% of the neurons ( $p < 0.001$  with respect to untreated controls) and neither the population of responding neurons (Figure 2.4A) nor the magnitude of the response (Figure 2.4B) increase when both stressors are added together. These findings suggest that a subpopulation of neurons is similarly sensitive to both A $\beta$ d/t and TNF $\alpha$ .

*TNF $\alpha$  initiates cofilin dephosphorylation.* Since only ~20% of A $\beta$ -treated neurons form rods and often rods are only within a few processes, changes in the levels of cofilin phosphorylation in response to A $\beta$  are below those detectable by immunoblotting methods (Maloney *et al.*, 2005). Thus an assay was developed based on the immunostaining of phosphorylated ADF/cofilin and total cofilin, and using ratio imaging to determine that cofilin dephosphorylation occurred in rod-forming neurites of neurons treated with A $\beta$  oligomer (Maloney *et al.*, 2005). We applied this method to determine if

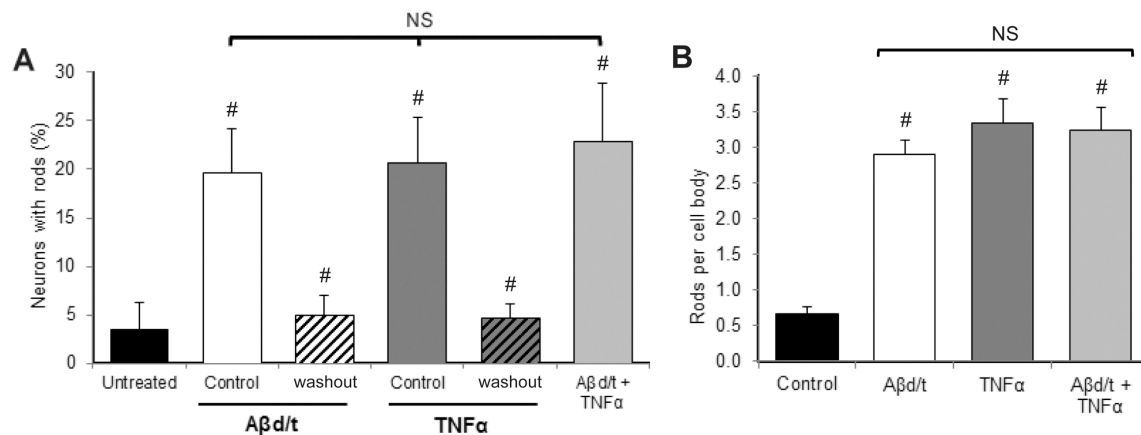


Figure 2.4: Rod formation in neurons in response to Aβd/t and TNFα used separately or together and their reversibility 24 h after washout. (A) Percent of neurons forming rods 24 h after treatment with Aβd/t (~250 pM) or TNFα (50 ng/ml) are the same and when used together there is no significant increase in response, suggesting that an identical population of neurons responds to both stimuli. Rods disappear by 24 h after removal (washout) of inducer. Treatments compared to the untreated control and washout compared to their treated controls are significant (# p<0.001). Differences in rod response between treatments are not significant (NS). (B) Rod numbers per cell body (rod index) between treatments are similarly significant (# p<0.001) from untreated control, but are not significant (NS) between the treatment conditions.

local changes in phosphorylated ADF/cofilin occurred within neurites in which rods formed when neurons were fixed at 2, 4, 8 and 12 h after TNF $\alpha$  treatment. Similar to what was observed for A $\beta$ -treated neurons, TNF $\alpha$  treatment led to cofilin dephosphorylation only in rod-containing neurites, with the highest levels of treatment was a gradual increase in dephosphorylated cofilin in the neurites containing a rod but outside of the rod region (Figure 2.5C number 2 and panel D neurites with rod). Neurites without rods (Figure 2.5C number 3) extending from neurons containing rods in other neurites showed no differences in the ratio image from those measured in non-rod forming neurons. From these data we were able to conclude that cofilin dephosphorylation in response to both TNF $\alpha$  and A $\beta$ d/t is highly localized to the neurites in which rods form.

*Rod persistence requires the presence of inducing agent.* We previously demonstrated that rods formed in neurons treated for 24 h with A $\beta$ d/t disappeared by 24 h after washout without neuronal loss (Davis *et al.*, 2011). Here we show that rods treated 12 h with TNF $\alpha$  are similarly reversed after 12 h washout (Figure 2.4A). However, to obtain more accurate measurements on the kinetics of rod disappearance, we utilized live cell imaging.

We determined whether or not cofilinR21Q-mRFP could be used to study the reversibility dynamics of A $\beta$ d/t- and TNF $\alpha$ -induced rods in real-time. Neurons were infected with adenovirus for expressing cofilinR21Q-mRFP and, after 36-48 h, treated with A $\beta$ d/t or TNF $\alpha$ . Individual neurons were randomly selected for imaging to follow rod

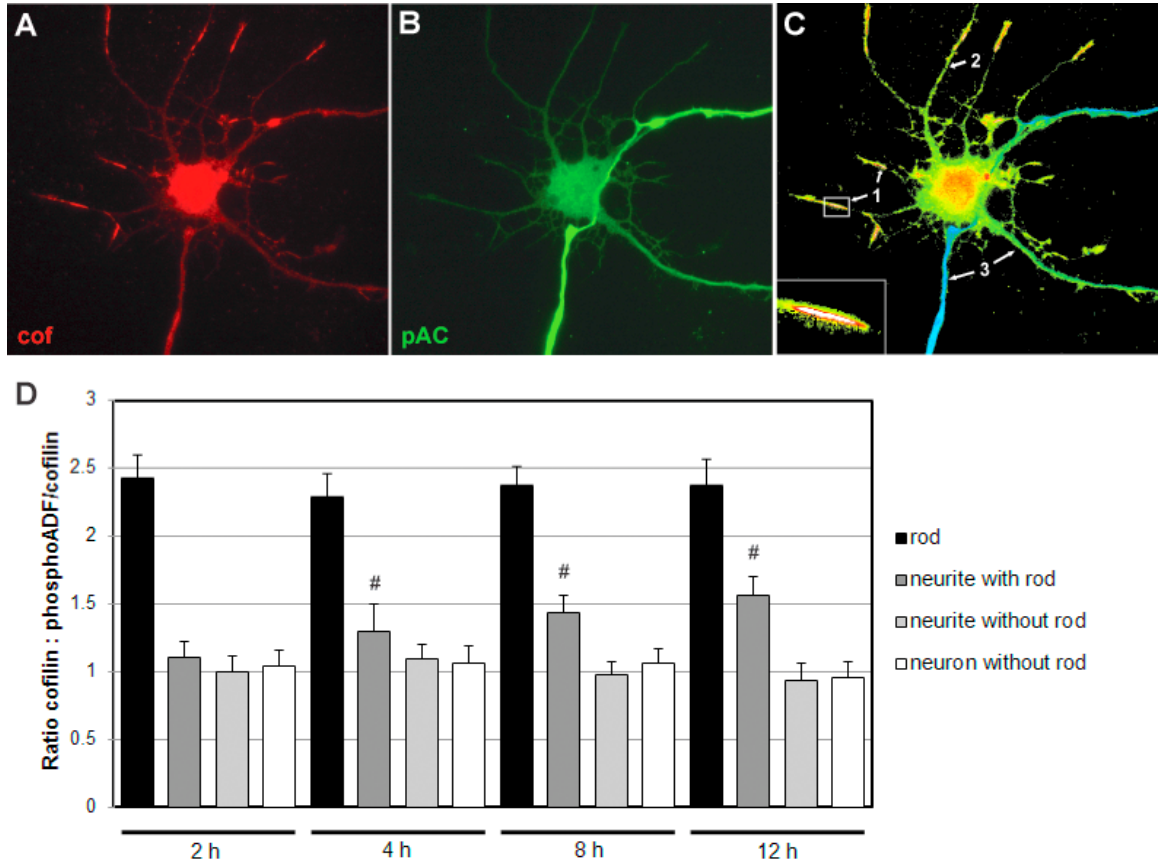


Figure 2.5: TNF $\alpha$  induces cofilin activation within neurites in which rods form but not in other neurites or neurons. Images of a neuron treated with TNF $\alpha$  for 8 h and fixed and immunostained for total cofilin (mouse antibody MAb22) and for phosphorylated ADF/cofilin (rabbit antibody). Example from a single neuron showing (A) total cofilin immunostaining, (B) phosphorylated ADF/cofilin immunostaining, (C) ratio image of total cofilin:phosphoADF/cofilin using a hot scale to show the regions of greatest activity (red/yellow). Numbers on the figure show the regions used to obtain: 1) ratio directly over rods, 2) ratio in a rod forming neurite but not in the rod region, 3) neurites without rods from a neuron with rods in other neurites. (D) Quantification of ratio images taken in different regions of neurons fixed at different times (2, 4, 8 and 12 h) after TNF $\alpha$  treatment. We observed a significant ( $\# p < 0.001$ ) increase in cofilin dephosphorylation by 4 h after TNF $\alpha$  treatment only in the region of a rod-containing neurite outside of the rod area.

formation for several hours. Previously we showed that neurons expressing cofilinR21Q-mRFP did not form new rods as a result of photo-stress of imaging (Mi *et al.*, 2013) (Figure 2.2B). TNF $\alpha$ -induced rod formation over 8 h is shown in Figure 2.6A. Rods sequester most of the cofilin within the processes in which they form as they elongate to their full length, which occurs within 20 min once initiated. Once rods enlarge to seemingly occlude the neurite, their mobility ceases. Despite occasional small rods observed undergoing translocation in the anterograde direction, newly formed rods predominantly move in the retrograde direction. They often disassemble and disappear as they near or enter the soma. The washout of TNF $\alpha$  resulted in the disappearance of induced rods with a half-life of 46 minutes (Figure 2.6C), reinforcing the dynamic nature of rods that depends on a minimum level of oxidative stress.

## Discussion

Here we show that cofilinR21Q-mRFP is a useful *in vivo* rod reporter and for the first time allows the visualization of induced rods and the dynamics of their disappearance after removal of the inducing agent.

Proinflammatory cytokines have been implicated in the progression of AD, as well as other chronic and acute neurodegenerative disorders and certain behavioral disorders (Cacquevel *et al.*, 2004; Amor *et al.*, 2010; Liu & Chan, 2014; McKee *et al.*, 2014). A $\beta$  increases proinflammatory cytokine release (Griffin & Barger, 2010) and proinflammatory cytokines also link TBI to later development of Alzheimer-type dementia (Sivanandam & Thakur, 2012; Breunig *et al.*, 2013). However, there appear to be contrasting cytokine profiles in extracts of frontal cortex from subjects with early AD,

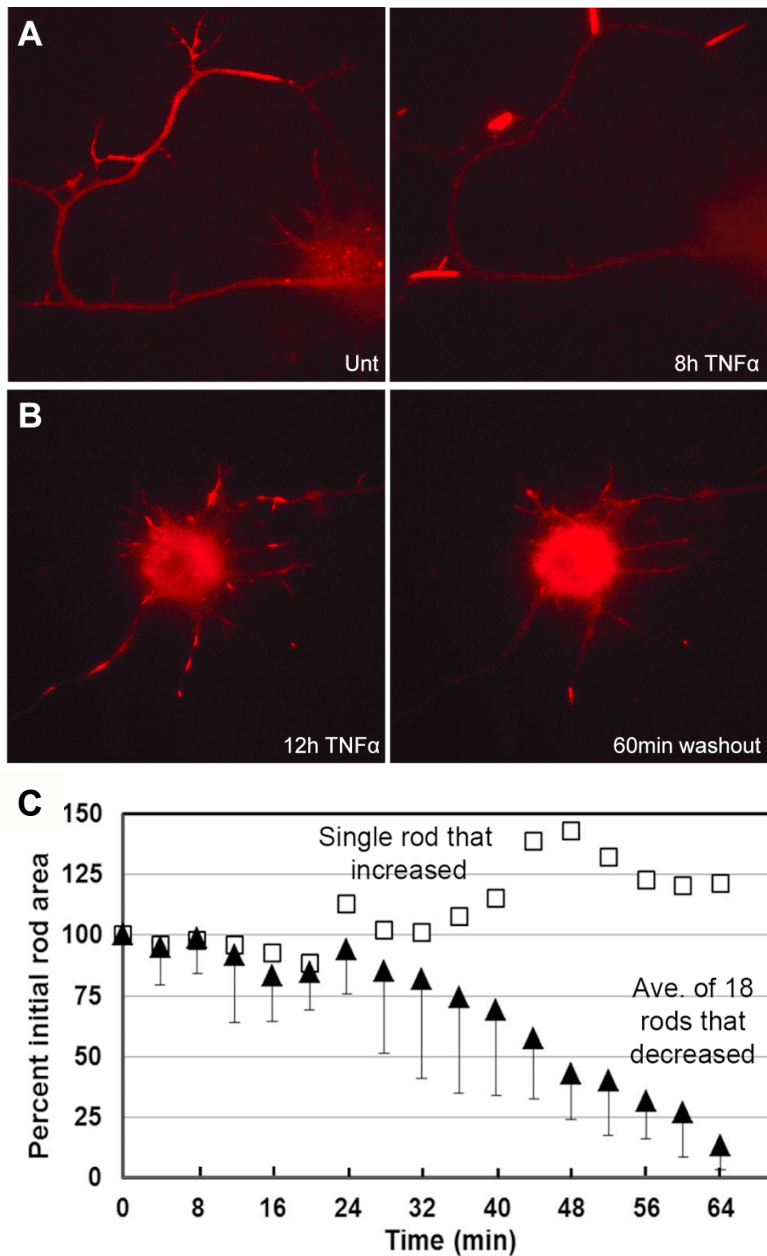


Figure 2.6: Rod dynamics and reversal observed in neurons using live cell imaging. Neurons infected with adenovirus expressing cofilinR21Q-mRFP 48 h prior to imaging. (A) Images of neurons untreated (left) or treated with TNF $\alpha$  for 8 h (right). (B) Image on left is a neuron treated for 12 h with TNF $\alpha$  in which rods have formed in many processes. Panel on right shows this same neuron 60 min after washout of the TNF $\alpha$  in which almost all rods have disappeared. (C) Time course of rod disappearance calculated from measurements on 5 rods per field from independent experiments. Total rod areas were quantified at 5 min intervals for washout of rod inducer to identify a half-life for disappearance of ~46 min.

one showing a preponderance of proinflammatory cytokines and the other showing elevated anti-inflammatory cytokines (Sudduth *et al.*, 2013). By end-stage AD, the phenotypes merge into one showing increase in both pro- and anti-inflammatory markers.

Finding different phenotypes in subjects suffering from early AD is not surprising given the multifactorial nature of sporadic AD (Orsucci D *et al.*, 2013). It is well established that amyloid plaques do not correlate with the severity of sporadic AD or cognitive status (Hernández & Avila, 2007; Scheff *et al.*, 2014). Furthermore, different cytokine profiles correlate with significant differences in abundance of extracellular amyloid plaques. Lower plaque numbers are found in subjects with elevated pro-inflammatory cytokines (Sudduth *et al.*, 2013), suggesting possible differences in the mechanism by which cognitive dysfunction develops in each subject cohort.

Polymorphisms in TNF $\alpha$  and in the promoter region of TNF $\alpha$  and IL-6 are associated with increased risk of AD and with late-onset sporadic AD (Vural *et al.*, 2009). TNF $\alpha$  stimulates NADPH oxidase (NOX) for ROS production in neurons (Barth *et al.*, 2012). A relationship between NOX activation and rod formation is described further in Chapter 3. ROS induce oxidation of 14-3-3 $\zeta$  in inhibitory complexes with Slingshot (SSH) (Kim *et al.*, 2009), a phosphatase that dephosphorylates (activates) cofilin. 14-3-3 $\zeta$  oxidation decreases its affinity for binding SSH, thereby releasing the active phosphatase to dephosphorylate cofilin. This suggests a possible ROS-mediated mechanism by which TNF $\alpha$  initiates both the dephosphorylation and oxidation of cofilin and therefore, rod formation.

CHAPTER 3:  
A CELLULAR PRION PROTEIN-DEPENDENT SIGNALING PATHWAY FOR NADPH  
OXIDASE ACTIVATION

**Introduction**

One binding partner for A $\beta$  is the cellular prion protein (PrP<sup>C</sup>) (Laurén *et al.*, 2009). A $\beta$ -mediated inhibition of long-term potentiation (LTP) (Barry *et al.*, 2011) and A $\beta$ -induced cognitive deficits in an AD mouse model (Chung *et al.*, 2010) are prevented by interrupting the A $\beta$ -PrP<sup>C</sup> interaction. PrP<sup>C</sup> is encoded by the *Prnp* gene that has highly conserved homologues across species (Figure 3.1) and which is expressed in highest amounts within neurons. The encoded protein from mouse contains 254 amino acids, 22 of which constitute the signal peptide removed from the N-terminus and 23 of which are in the C-terminal peptide removed upon glycosphosphatidylinositol (GPI) linkage to residue 231. The N-terminal signal peptide is followed by four to five octapeptide repeats. Copper binding at these five sites induces significant conformational changes to the prion protein, which may have important implications in modulating PrP<sup>C</sup> interactions with other membrane proteins (You *et al.*, 2012). The C-terminal region preceding the GPI anchor that links the C-terminus to the outer lipid leaflet of the plasma membrane contains three  $\alpha$ -helices (Stahl *et al.*, 1992; Aguzzi & Heikenwalder, 2006).

PrP<sup>C</sup> contains two potentially glycosylated asparagine residues (Ermonval *et al.*, 2003) and undergoes three different proteolytic cleavages (Aguzzi & Heikenwalder, 2006). Thus, cellular prion exists as a number of post-translationally modified isoforms

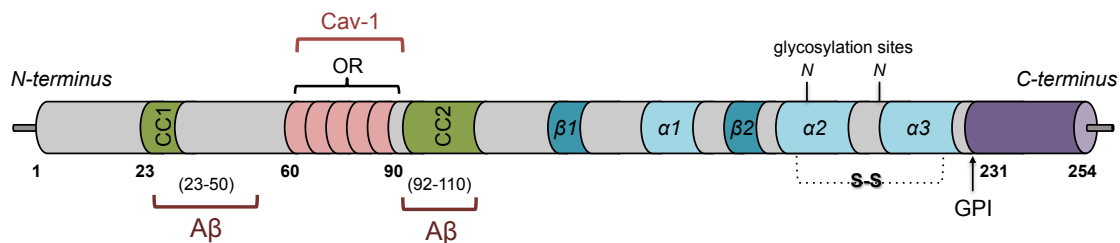


Figure 3.1: Secondary structure and interactions of the cellular prion protein. PrP<sup>C</sup> contains two charged clusters (CC1/2) on either side of five copper-binding octapeptide repeats (OR). Two principal binding sites have been identified for A $\beta$  (23-50 and 92-110) whereas caveolin-1 has been shown to interact with ORs, where it may serve to link cellular prion to the activation of fyn tyrosine-kinase. The C-terminal domain contains three alpha helices, two of which are stabilized by a disulfide bond, while a third ( $\alpha$ 1) unfolds and is converted to the PrP<sup>Sc</sup> conformation. GPI at amino acid 231 anchors PrP<sup>C</sup> to the extracellular leaflet of the plasma membrane.

whose distribution and relevance may vary based on distinct brain region or cell type. This concept of prion speciation might account for its role in a spectrum of neurodegenerative disorders that include AD, Parkinson and Huntington diseases, infectious PrP<sup>Sc</sup> prionopathies, TBI, and other frontotemporal dementias such as chronic traumatic encephalopathy (CTE) (Prusiner, 2013; Renner & Melki, 2014).

The soluble form of TNF $\alpha$  is produced from its parental membrane protein upon activation of TNF $\alpha$  converting enzyme (TACE), a process that can be initiated by PrP<sup>C</sup>-mediated synthesis of ROS (Pradines *et al.*, 2009). Furthermore, TACE enhances the  $\alpha$ -cleavage of PrP<sup>C</sup>, which prevents its conversion into the misfolded PrP<sup>Sc</sup> (Hernandez-Rapp *et al.*, 2014). This suggests a possible feed-forward mechanism for activating more soluble TNF $\alpha$  and signaling via PrP<sup>C</sup>.

PrP<sup>C</sup>-dependent signaling pathways have been shown to activate NADPH oxidase (NOX) (Krause *et al.*, 2012), a ROS-producing family of seven isoforms named for their largest subunit, several of which are present in neuronal cells (Serrano *et al.*, 2003; Lambeth, 2004; Vallet *et al.*, 2005). NOX2, also known as gp91<sup>phox</sup>, is described in a variety of tissues, including neurons in the hippocampus and other regions of the neuraxis (Serrano *et al.*, 2003). Its activation requires phosphorylation-dependent localization of p47<sup>phox</sup> to the membrane and contact with gp91<sup>phox</sup> and p22<sup>phox</sup>. This interaction permits contact of p67<sup>phox</sup> with gp91<sup>phox</sup>, and interaction with the small regulatory GTPase Rac1 or Rac2 (Figure 3.2) (Groemping & Rittinger, 2005; Hordijk, 2006). These NOX isoforms generate ROS via assembly of subunits at the plasma membrane in concert with lipid activators such as ceramide metabolites and arachidonic

acid (Sumimoto, 2005; Barth *et al.*, 2012), resulting in the transfer of electrons from cytosolic NADPH to oxygen (Bedard & Krause, 2007; Krause *et al.*, 2012).

Here we determine that A $\beta$  and proinflammatory cytokines induce the PrP<sup>C</sup>-dependent activation of NOX to generate ROS. An oxidizing environment initiates cofilin-actin rod formation that is reversible by interrupting NOX activity. Surprisingly, PrP<sup>C</sup> overexpression is sufficient to induce rods in a NOX-dependent manner, suggesting a common mechanism by which multiple and functionally diverse A $\beta$ -binding membrane proteins might cause synaptic dysfunction.

## Materials and Methods

*Neuronal Cell Culture.* Rat E18 cortical and hippocampal neurons were obtained, prepared and maintained as described in Chapter 2.

*Adenovirus Preparation.* Adenoviruses were made using the AdEasy system (He *et al.*, 1998; Minamide *et al.*, 2003). pShuttle CMV was used to make adenoviruses for expression of lacZ-GFP or mRFP (for control infections), cofilinR21Q-mRFP, EGF-PrP<sup>C</sup> (or EGFP-linked via a GPI group to membrane), p47-roGFP and DNp22<sup>phox</sup>. The EGFP-PrP<sup>C</sup> coding region was cut from the wt plasmid containing mouse PrP<sup>C</sup> in the pEGFP-C1 vector (Haigh *et al.*, 2005). The EGFP-GPI control came from the same plasmid with the PrP<sup>C</sup>-coding region removed. Briefly, the coding regions were excised with NheI/SmaI, and ligated into the XbaI/EcoRV sites of pShuttleCMV. A reporter for NADPH oxidase activity was generated by linking redox-sensitive GFP (roGFP) to the NOX organizer protein, p47<sup>phox</sup>, as described by Pal *et al.*, 2013 (generous gift from

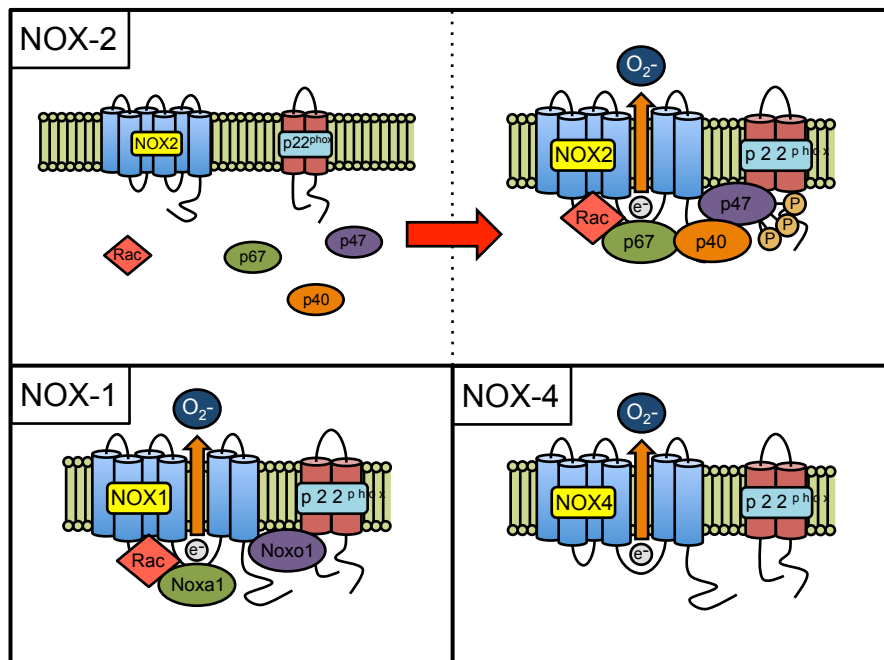


Figure 3.2: Neuronal NOX isoforms and assembly. NADPH oxidase is a family of seven isoforms that generate ROS. NOX-1, 2, and 4 have all been identified in neuronal cells. Assembly of NOX-2 requires the phosphorylation-dependent localization of p47<sup>phox</sup> to the membrane and contact with NOX2 (gp91<sup>phox</sup>) and p22<sup>phox</sup> subunits. Contact with p67<sup>phox</sup> and interaction with Rac1/2 GTPase shuttles an electron from cytosolic NADPH to oxygen (adapted using Bedard & Krause, 2007)

George Rodney, Baylor College of Medicine). Adenoviruses for expression of cofilinR21Q-mRFP in pShuttle behind a CMV promoter have been described above (Mi *et al.*, 2013). Adenoviruses for expressing the proteins were then made and titered (Minamide *et al.*, 2003).

*Characterization of Adenoviruses.* EGFP-PrP<sup>C</sup> and p47-roGFP adenoviruses were tested for expression of the encoded protein by infection of either SAOS2 or N2a cells, waiting until fluorescence was readily visible in at least 50% of the cells (~36-48 h postinfection). Cells were then washed and lysed in an SDS-lysis buffer (Morgan *et al.*, 1993) and Western blots were performed using antibodies against the protein of interest and GAPDH as an internal standard for normalization. Chimeric proteins with EGFP had migration mobility equivalent to a mass of about 25 kDa above the endogenous non-chimeric protein. Experiments were usually performed 60-72 h after infection for expressing fluorescent proteins either as chimeras or infection markers.

### *Cell Treatments*

Adenovirus infection. Cells were infected on day 2 for 60 h with 30-100 MOI EGFP-PrP<sup>C</sup> adenovirus and/or on day 3 for 40 h with 150 MOI cofilinR21Q-mRFP (CMV) adenovirus. Infection on day 3 for 36 h with 100 MOI p47-roGFP was used for detecting ROS production via changes in roGFP fluorescence.

Rod inducing treatments. For rod induction, cells were treated with A $\beta$ d/t, TNF $\alpha$ , IL-1 $\beta$ , or IL-6 (prepared as described previously), dissolved in Neurobasal medium at 100x the final concentration used in culture. Rods were also induced by medium addition to a final concentration of 2  $\mu$ M antimycin A or 100  $\mu$ M glutamate, or by an incubation of neurons in PBS containing 10 mM NaN<sub>3</sub>/6 mM 2-deoxy-D-glucose (ATP depletion), all

for 30 min prior to fixation. Cell cultures with a medium change prior to the day of fixation served as controls.

*Reagent Preparation.* A NOX-1/2-isoform inhibitor (TG6-227, EC<sub>50</sub> 200 nM) was obtained from Dr. J. David Lambeth (Emory University). 10.4 mg TG6-227 (MW ~330) was brought up in 31.25  $\mu$ l DMSO (1 M) and stored at 210 mM (-80°C). TG6-227 was diluted in Neurobasal medium and used at 1  $\mu$ M. 2-Acetylphenathiazine (ML171) was dissolved in DMSO at 100 mM and used at 500 nM and apocynin was dissolved in DMSO to 1 mM and used at 1  $\mu$ M in culture. The usual vehicle control was DMSO at 0.1% final concentration but in some experiments DMSO was used at 1% without detrimental effects over 12 h. Cell cultures were pretreated with NOX inhibitors for 1-2 h prior to treatment with glutamate, antimycin A, A $\beta$ d/t, or TNF $\alpha$ .

*Fixation and Immunolabelling.* Cells were fixed and immunostained for cofilin-actin rods as described previously (Chapter 2). Additionally, Alexa 488-CTxB was used to observe dynamics of membrane Gm1 ganglioside at sites of rod formation, as described by Mi *et al.*, 2013 and illustrated in Figure 3.3.

*Western Blot.* To ensure that genetic knockout of PrP<sup>C</sup> was not having an effect on NOX-1/2 expression, western blots of both PrP<sup>C</sup>-null and wildtype whole hippocampus and cortex were performed.

*Imaging and Analysis and Statistics* were performed as described in Chapter 2.

## Results

*PrP<sup>C</sup> is required for A $\beta$ d/t, TNF $\alpha$ , IL-1 $\beta$  & IL-6-induced rods.* If indeed rods are a plausible mechanism for the synapse dysfunction induced by A $\beta$ d/t, then there should

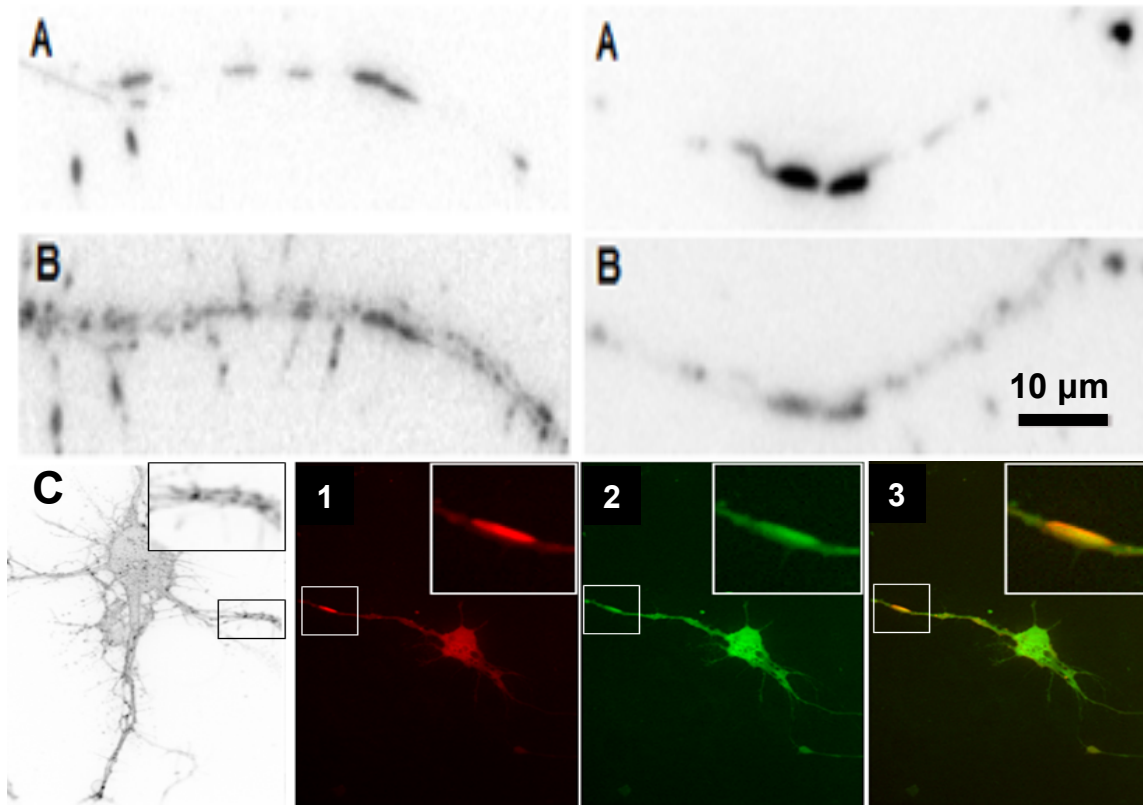


Figure 3.3: CTxB-stained lipid rafts. Fluorescent labeled CTxB binds Gm1 gangliosides of distinct LR micodomains. (A) Rods immunostained for ADF/cofilin (Alexa 594) in two random neurons exposed to A $\beta$ d/t. (B) Cells were subsequently incubated 15 min with Alexa 488-CTxB. This crude trial experiment revealed that rods colocalized with LR domains to an extent (Bamburg, unpublished data). (C) Inverted fluorescence image showing puncta of Alexa 488-CTxB staining in control neuron (left). A cofilinR21Q-mRFP expressing neuron was treated 6 h with TNF $\alpha$  to induce a rod (1) and incubated 15 min with Alexa 488-CTxB (2). Overlay (3) shows lipid raft coalescence occurs over the region of the rod. Insets are magnifications of boxed areas. Rod (1-3) is 5  $\mu$ m (Mi, 2013 Master's thesis).

be a dependence on PrP<sup>C</sup> for their formation induced by A $\beta$ . We cultured hippocampal neurons from PrP<sup>C</sup>-null mice (P0) and compared rod formation in response to A $\beta$ d/t (250 pM) and the proinflammatory cytokines (each at 50 ng/ml) to hippocampal neurons from P0 wild type (wt) mice of the same line (FVB). Neurons from wt mice showed the expected 20-25% rod response (Figure 3.4A), whereas rod formation in PrP<sup>C</sup>-null neurons was significantly reduced to that of untreated controls ( $p < 0.01$  for A $\beta$ d/t TNF $\alpha$ , and IL-1 $\beta$ ;  $p < 0.05$  for IL-6). Excitotoxic glutamate (~85%) and ATP-depletion (~98%) (addition of mitochondrial inhibitors with or without the glycolysis inhibitor 2-deoxy-D-glucose) both prompt a robust rod response in neurons (Figure 3.4). Importantly, we found that neither of these stresses depends upon the presence of PrP<sup>C</sup>. These findings demonstrate that the hippocampus of both rats and mice have a similar subpopulation of neurons that forms rods with the same inducing agents and that there are at least two independent pathways leading to rod formation in hippocampal neurons.

*PrP<sup>C</sup> overexpression is sufficient for rod formation.* PrP<sup>C</sup> is linked via a GPI lipid anchor to the membrane outer leaflet where it has been shown to interact with A $\beta$  (Laurén *et al.*, 2009). The mechanism(s) by which cellular prion participates in signal transduction, including NOX activation, is not well understood. Since A $\beta$ -induced synaptic damage can be mediated by the cross-linking of PrP<sup>C</sup> (Bate & Williams, 2011), we determined if overexpression of PrP<sup>C</sup>, and hence increased density within membrane domains, alone could be sufficient to induce rod formation. To test this, we infected cultured hippocampal neurons with adenovirus expressing EGFP-PrP<sup>C</sup> driven

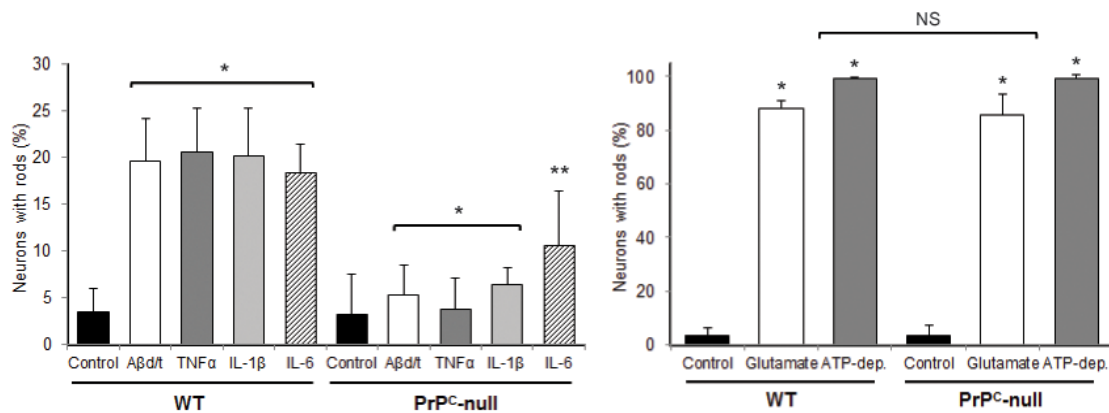


Figure 3.4: PrP<sup>C</sup> is required for rod formation from Aβ<sub>d</sub>/t and proinflammatory cytokines, but not from rods induced by glutamate or mitochondrial inhibitors. (A) Percent of neurons with rods 20 h after treatment with Aβ<sub>d</sub>/t or proinflammatory cytokines measured in dissociated neurons from FVB wild type mice or from the PrP<sup>C</sup>-null mouse made in the FVB background. All of the decreases in the response of PrP<sup>C</sup>-null neurons are significant with respect to their wild type controls (\* p<0.001; \*\* p<0.005). (B) Rod formation is significant (\* p<0.001) with respect to untreated neurons but does not differ significantly (NS) between hippocampal neurons from wild type (WT) and PrP<sup>C</sup>-null mice in response to excitotoxic levels of glutamate (150 μM) or ATP-depletion (10 mM NaN<sub>3</sub>, 2 mM 2-deoxyglucose) demonstrating that neither of these rod-inducing stresses utilize a PrP<sup>C</sup>-dependent pathway.

by a strong CMV promoter. Results from previous studies using this construct demonstrated that EGFP-PrP<sup>C</sup> reached the cell surface (Haigh *et al.*, 2005).

We infected rat hippocampal neurons at different MOIs with EGFP-PrP<sup>C</sup> compared to control adenovirus expressing GFP. Neurons infected with 100 MOI of adenovirus expressing GFP alone had no increase in rods over untreated controls. Of EGFP-PrP<sup>C</sup> positive neurons infected at an MOI of 30, 19% had rods ( $p < 0.001$  compared to control) and this percentage significantly increased when neurons were treated with TNF $\alpha$  (31%,  $p < 0.005$ ) or A $\beta$ d/t (37%,  $p < 0.001$ ) (Figure 3.5A). When neurons were infected with an MOI of 100, 40% of GFP positive cells contained rods (significant at  $p < 0.001$  compared to untreated controls) but the slightly increased responsiveness to TNF $\alpha$  or A $\beta$ d/t treatment was no longer significant (Figure 3.5A). Therefore, PrP<sup>C</sup> overexpression alone can induce rods to a level upon which external stimulus no longer has a significant additional effect.

To determine if neurons from PrP<sup>C</sup>-null mice would form rods upon re-expressing PrP<sup>C</sup>, we compared rod formation between wt and PrP<sup>C</sup>-null hippocampal neurons infected with different MOIs of the EGFP-PrP<sup>C</sup> adenovirus. Both A $\beta$ d/t and TNF $\alpha$  induced rods in the wt but not in the PrP<sup>C</sup>-null neurons (Figure 3.5B). Spontaneous rod formation occurred to about the same degree in either genotype and infection with EGFP-PrP<sup>C</sup> at an MOI of 10 had no significant effect. However, at MOIs of 30 or 100, rod formation was significantly ( $p < 0.001$ ) enhanced in wt and PrP<sup>C</sup>-null neurons. Addition of A $\beta$ d/t or TNF $\alpha$  to neurons of either genotype infected with 100 MOI did not result in any significant increase in rod formation (Figure 3.5). These results demonstrate both the necessity of PrP<sup>C</sup> for rod formation induced by A $\beta$ d/t or TNF $\alpha$  and

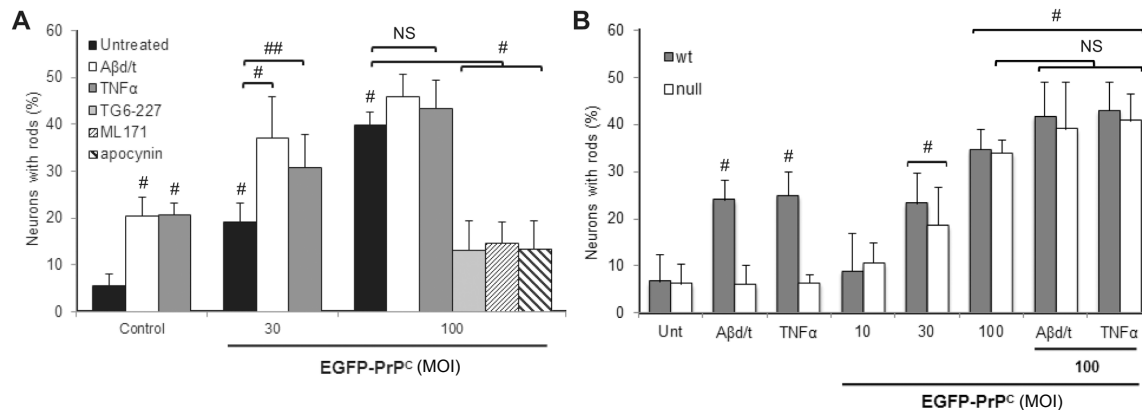


Figure 3.5: PrP<sup>C</sup> overexpression induces rods in both rat and mouse neurons and requires NOX for rod formation. (A) E18 rat hippocampal neurons infected with adenovirus expressing EGFP alone (control; 100 MOI) or EGFP-PrP<sup>C</sup> (30 and 100 MOI) for 60 h were left untreated or treated with Aβd/t or TNFα (20 h) prior to fixing, immunostaining and quantifying the percent of neurons with rods. Neurons infected (100 MOI) with adenovirus for expressing EGFP-PrP<sup>C</sup> for 60 h were left untreated or treated with the NOX inhibitors at the concentrations used in *Figure 3.9* for 4 h prior to fixation and rod quantification. Within each group, treatments are compared for significance (# p<0.001; ## p<0.005) with respect to the group control (black column). Significance of the EGFP-PrP<sup>C</sup> infected groups are compared to the untreated control (# p<0.001). (B) P0 hippocampal neurons were obtained from wt and PrP<sup>C</sup>-null FVB pups and plated neurons on day 5 were left untreated or treated with Aβd/t or TNFα as previously described. Some cultures were infected on day 3 with different MOIs of adenovirus for expressing EGFP-PrP<sup>C</sup> and after 60 h some of the cultures infected with 100 MOI of virus were also treated with Aβd/t or TNFα. PrP<sup>C</sup>-null neurons did not form rods in response to Aβ or TNFα but both wt and PrP<sup>C</sup>-null neurons responded identically by forming spontaneous rods when infected with 30 or 100 MOI of PrP<sup>C</sup>-expressing adenovirus (# p<0.001 from uninfected control).

also the sufficiency of the PrP<sup>C</sup> overexpression alone for rod formation.

Furthermore, we showed that EGFP-PrP<sup>C</sup> aggregated in distinct patches over regions in which rod formation was also observed. Neurons infected with a low (30) MOI of EGFP-PrP<sup>C</sup> adenovirus were observed over a time course of A $\beta$ d/t treatment (Figure 3.6). The aggregation of PrP<sup>C</sup> (arrows) coincided with regions of rod formation; however, it is unclear whether this supports our hypothesis of PrP<sup>C</sup> coalescence in enlarged membrane domains or rather that PrP<sup>C</sup>-containing vesicles stalled at regions where rods formed.

To ensure that PrP<sup>C</sup> expression was not having an indirect effect on rod formation through cytokine secretion and a possible autocrine feedback loop, we performed a multiplex assay for 11 cytokines, including all three of the ones tested for rod induction (Figure 2.3), in medium collected from high density neuron cultures prepared from PrP<sup>C</sup>-null mice. Some cultures were infected with different MOIs of adenovirus for EGFP-PrP<sup>C</sup> expression to determine if re-expression of cellular prion to levels that induced rods in up to 40% of neurons (100 MOI, Figure 3.5A) also had an impact on overall cytokine secretion. The sensitivity of the assay was demonstrated to detect each cytokine at least one order of magnitude below the level required to obtain a minimal rod response (1.5 ng/ml in Figure 2.3). All 11 cytokines in the medium from both uninfected and infected PrP<sup>C</sup>-null neuronal cultures (100 MOI) were below a detectable level, indicating that this possible indirect role of PrP<sup>C</sup>-induced cytokine secretion need not be considered further.

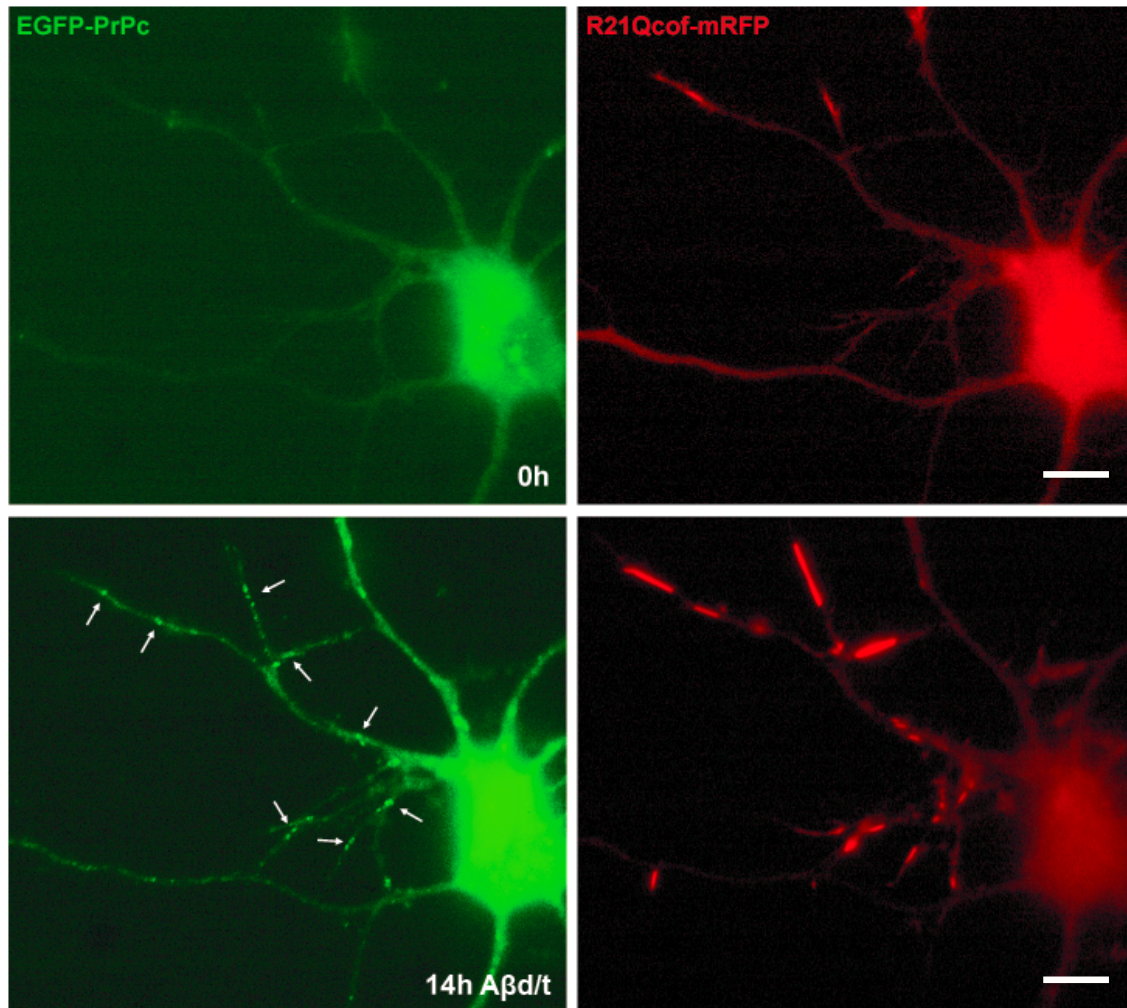


Figure 3.6: Cofilin-actin rod formation co-localizes with distinct PrP<sup>C</sup> patches. E18 rat hippocampal neurons were infected with EGFP-PrP<sup>C</sup> (30 MOI) adenovirus for 60 h and observed over the time course of A $\beta$ d/t treatment. Rod formation was visualized using an R21Q cofilin-mRFP (150 MOI) (40 h) adenovirus, a mutant form of cofilin that incorporates only into stress-induced cofilin-actin rods. Rod formation coincided with the emergence of several distinct PrP<sup>C</sup> labeled patches after 14 h exposure to A $\beta$ d/t. However, this could have been a result of rods stalling PrP<sup>C</sup>-containing vesicles within neurites. Live-cell imaging was done using total internal reflection fluorescence (TIRF) microscopy with a 60X objective. Standard bar = 10  $\mu$ m.

*NOX inhibition prevents A $\beta$ d/t- and TNF $\alpha$ -induced rod formation.* Oxidative stress markers in the brain increase during early stages of cognitive impairment (Keller *et al.*, 2005) and correlate with enhanced NOX activity (Ansari & Scheff, 2011). To first determine that prion knockout mice had no effect on expression of the major NOX isoforms, NOX-1 and NOX-2, immunoblots were performed which showed no change in their expression in extracts from wt and PrP<sup>C</sup>-null mouse brain (Figure 3.7).

To test the hypothesis that NOX activity and subsequent ROS production is required for PrP<sup>C</sup>-dependent rod formation, we used both dominant interfering and various pharmacological approaches to block NOX, for which isoforms 1, 2 and 4 have been identified in CNS neurons (Lambeth, 2004; Bedard & Krause, 2007; Sorce & Krause, 2012). The P156Q mutation in the NOX subunit p22<sup>phox</sup> exerts a dominant negative (DN) effect preventing the recruitment of Nox1/ p47<sup>phox</sup> subunits and rendering NOX isoforms 1–3 inactive (Sorce & Krause, 2009; Krause *et al.*, 2012). We generated a replication-deficient, recombinant adenovirus to co-express DNp22<sup>phox</sup> and green fluorescent protein (GFP) under separate promoters (Ad-DNp22<sup>phox</sup>) (He *et al.*, 1998).

The ability of expressed DNp22<sup>phox</sup> to prevent the increase in ROS induced by phorbol myristate acetate (PMA) treatment was tested using the osteosarcoma SAOS2 cell line using oxidation of 2',7'-dihydrodichlorofluorescein (DCF) as a measure of ROS (Barth *et al.*, 2009). Uninfected and virus control (mRFP alone) infected cells responded identically to PMA whereas the increase in ROS due to PMA was inhibited by DNp22<sup>phox</sup> (Figure 3.8A).

Dissociated hippocampal neurons were infected with Ad-DNp22<sup>phox</sup> or a GFP-

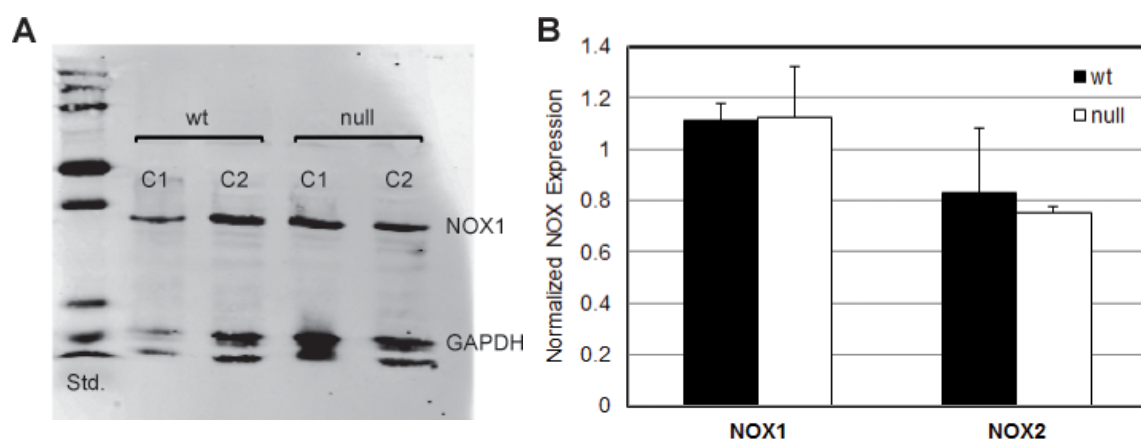


Figure 3.7: Brain expression levels of NOX1 and NOX2 are similar in wild type and PrP<sup>C</sup>-null mice. (A) Typical western blot of extracts from the cortex of two wt and two PrP<sup>C</sup>-null FVB mice showing bands for NOX1 and GAPDH. (B) Quantitative information from duplicate blots of duplicate extracts in which intensities of NOX1 and NOX 2 bands were normalized to GAPDH. There are no significant differences of in the brain expression levels of NOX1 and NOX2 between wt and PrP<sup>C</sup> null mice. Bars = std. deviation.

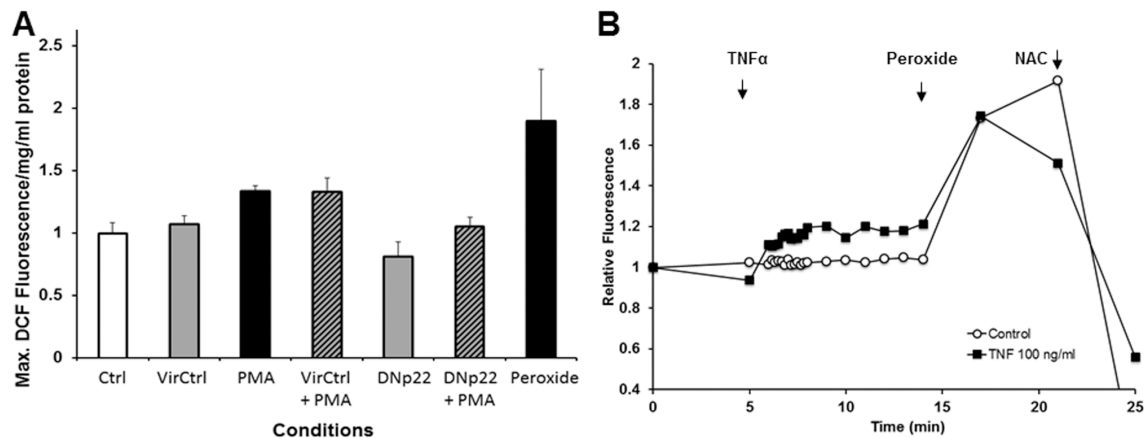


Figure 3.8: DCF analysis for ROS visualization. (A) SAOS2 cells were kept uninfected (Ctrl) or infected with a control adenovirus (VirCtrl) or with adenovirus for expressing DNp22<sup>phox</sup>. After 48 h, cells were loaded with DCF-diacetate (20  $\mu$ M) for 1 h, washed, and then left untreated or treated with phorbol myristate acetate (PMA; 400 ng/ml) or peroxide (500  $\mu$ M) for 30 min before lysis and quantification of lysate for fluorescence and protein. Infection with control virus had no effect on the ability of the cells to generate a ROS response to PMA but expression of DNp22<sup>phox</sup> inhibited the response. The peroxide positive control shows the maximum changes that could be detected in this assay. (B) Changes in intracellular DCF fluorescence measured over the soma of two neurons 5 min before and at 10–30 sec intervals for 10 min after treatment with 100 ng/ml TNF $\alpha$ . Average intensity per unit area is normalized to pretreatment values at 0 time. In multiple experiments (n = 9) using either 100 ng/ml of 50 ng/ml TNF $\alpha$ , 19 out of 69 (27%) cells imaged over time showed a DCF fluorescence response similar to the responding cell and the other 50 showed no response (labeled here as control). After 10 min, peroxide was added to 500  $\mu$ M to demonstrate a positive response in every cell and about 5 min later excess reducing agent (1 mM N-acetylcysteine; NAC) was added to reverse the oxidative response.

expressing adenovirus as a control. After 48 h, neurons were treated for 20 h with either A $\beta$ d/t (250 pM) or TNF $\alpha$  (50 ng/ml), fixed, immunostained for cofilin (Alexa 594 secondary antibody), and GFP-positive neurons were scored for rod formation. A $\beta$ d/t- and TNF $\alpha$ -treated neurons infected with the control viruses formed rods to the same extent as uninfected cells (included in controls) and were significantly ( $p < 0.001$ ) above untreated neurons. In contrast, rod formation in neurons expressing DNp22<sup>phox</sup> was indistinguishable from untreated controls (Figure 3.9).

We also tested three different pharmacological inhibitors of NOX for their ability to inhibit rod formation induced by A $\beta$ d/t, TNF $\alpha$  or glutamate. TG6-227 inhibits NOX-1 and -2 with an IC<sub>50</sub> of 200 nM but does not inhibit NOX-3 or -4 (unpublished results from J.D. Lambeth). 2-Acetylphenathiazine (ML171) inhibits NOX-1 with an IC<sub>50</sub> of about 200 nM but has a 10–20 fold higher IC<sub>50</sub> for NOX-2 and -3 (Altenhoffer *et al.*, 2014). Apocynin is a broad spectrum NOX inhibitor with other off-target effects (Mo *et al.*, 2014). When used at 3– 10 fold above their IC<sub>50</sub> value for their most specific NOX isoform target, all of these NOX inhibitors significantly ( $p < 0.001$ ) reduced rod formation to that of untreated controls in both A $\beta$ d/t- and TNF $\alpha$ -treated neurons but did not affect rod formation in response to excitotoxic levels of glutamate (Figure 3.9). Although some of these NOX inhibitors may have other NOX-independent targets, taken together with the effects of DNp22<sup>phox</sup>, these results strongly suggest that A $\beta$ d/t and TNF $\alpha$ , but not glutamate, induce rods through a pathway dependent upon NOX activity.

*A $\beta$ d/t and TNF $\alpha$  stimulate ROS generation in neurites.* Once we confirmed that prion-dependent rod formation utilizes NOX activity, we used both DCF and a redox-

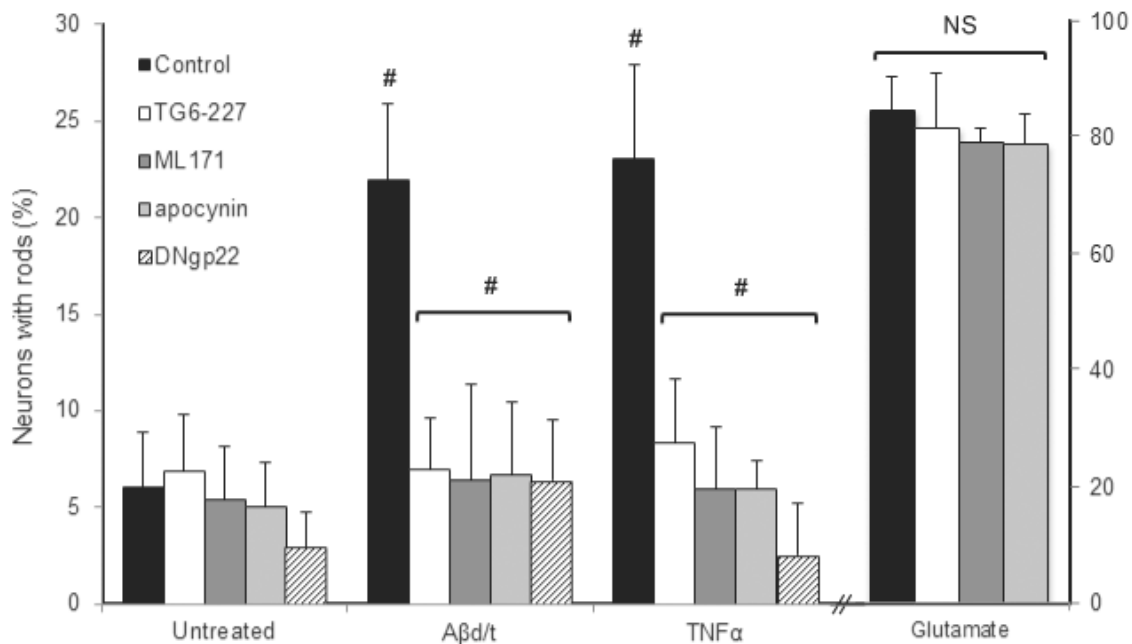


Figure 3.9 Aβd/t and TNFα utilize a NOX-dependent pathway for rod formation. Hippocampal neurons were either untreated or infected with adenovirus for expressing DNp22PHOX for 48 h prior to day 5 in culture. Some cultures were pre-treated 1 h with NOX inhibitors TG6-227 (1 μM), ML171 (500 nM) or apocynin (1 μM). In the continued presence of the NOX inhibitors (or in neurons expressing DNp22 for 48 h), neurons were treated for 20 h with Aβd/t (~250 pM) or TNFα (50 ng/ml), or for 30 min with glutamate (150 μM) before fixing, immunostaining for cofilin and quantifying the percent of neurons with rods. Rod response to Aβd/t and TNFα, but not glutamate, was significantly (# p<0.001) reduced by each of the NOX inhibitors.

sensitive NOX subunit (p47-roGFP) to test for ROS generation within neurons. The visualization of DCF oxidation by fluorescence microscopy was used to demonstrate that TNF $\alpha$  stimulated ROS production in a subpopulation (about 27%) of rat hippocampal neurons. The early time course of a responding neuron and a non-responding neuron in the same culture is shown in Figure 3.8B with effects of peroxide (positive oxidizing control) and N-acetylcysteine (NAC) (reducing control) also shown. Measurements were made over the soma because neurites were too faint to measure. Neurons were also infected 36 h with the redox-sensitive p47-roGFP adenovirus and time course of A $\beta$ d/t and TNF $\alpha$  was observed using TIRF microscopy. Similar to visualization of DCF, both stressors increased detectable ROS levels, but with an intensity that allowed measurements of individual neurites. The fluorescence of roGFP was sensitive to both peroxide and NAC additions (Figure 3.10). Random neurons were chosen but only 27% were responsive to ROS-inducing treatment, of which only 52% of neurites exhibited an increased fluorescence in roGFP measurements over time.

*NOX inhibition reverses prion-dependent rods.* We also studied the reversal of rods formed in neurons overexpressing PrP<sup>C</sup>. In these neurons, we significantly ( $p < 0.001$ ) reversed rod formation by addition of the NOX inhibitors TG6-227, ML171 and Apocynin (Figure 3.5A). Furthermore, we observed the reversal of rods in live cells formed by PrP<sup>C</sup> overexpression using TG6-227 and ML171, as shown in Figure 3.11. The rate of rod reversal with addition of NOX inhibitors is slightly faster than that measured upon washout of the rod inducers (Figure 2.6C), suggesting that continued

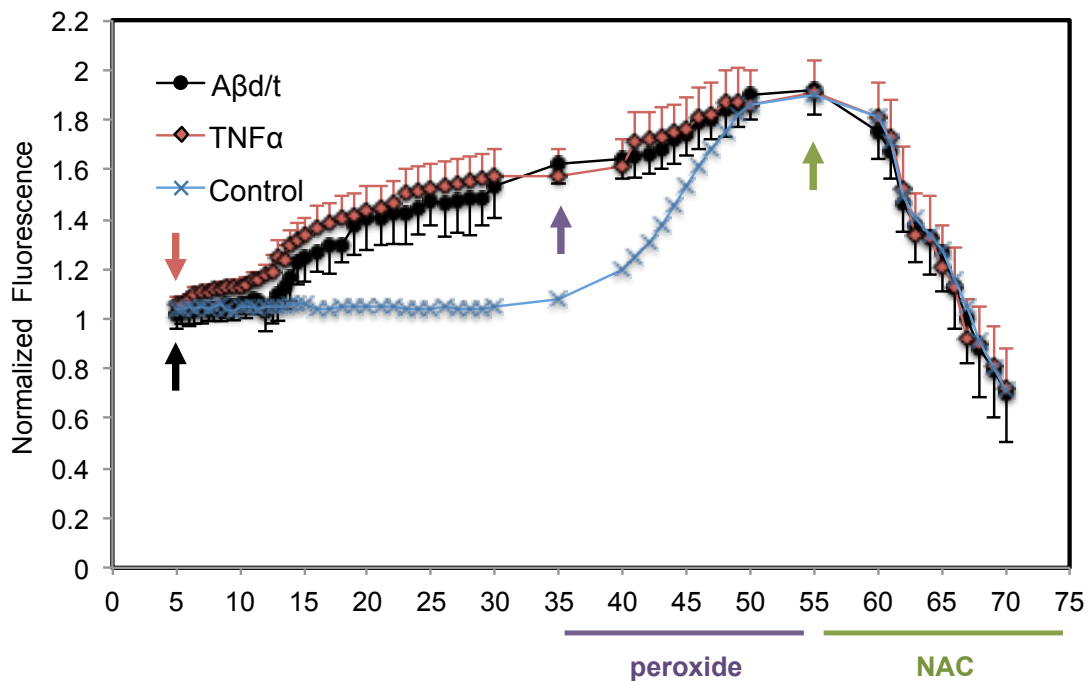


Figure 3.10: Aβd/t and TNFα initiate the generation of ROS in neurites. Neurons were infected 36 h with the redox-sensitive p47-roGFP adenovirus and fluorescence was measured in random neurites. In multiple experiments, time course of ROS production was measured after addition of 250 pM Aβd/t or 100 ng/ml TNFα and was observed as increased fluorescence of 488 nm excitation using TIRF microscopy. Only in neurons that were responsive to increased ROS for both Aβd/t (15 out of 54 neurons, 27.8%) and TNFα (15 out of 56 neurons, 26.8%) were neurites examined individually (90 out of 173 total neurites measured, 52%). Responsive neurites were compared to untreated control neurites from various experiments that did not increase roGFP fluorescence. After 35 min, peroxide (500 μM) was added to demonstrate a positive response in all neurites and about 20 min later excess reducing agent (1 mM NAC) was added to reverse the oxidative response in all neurites.

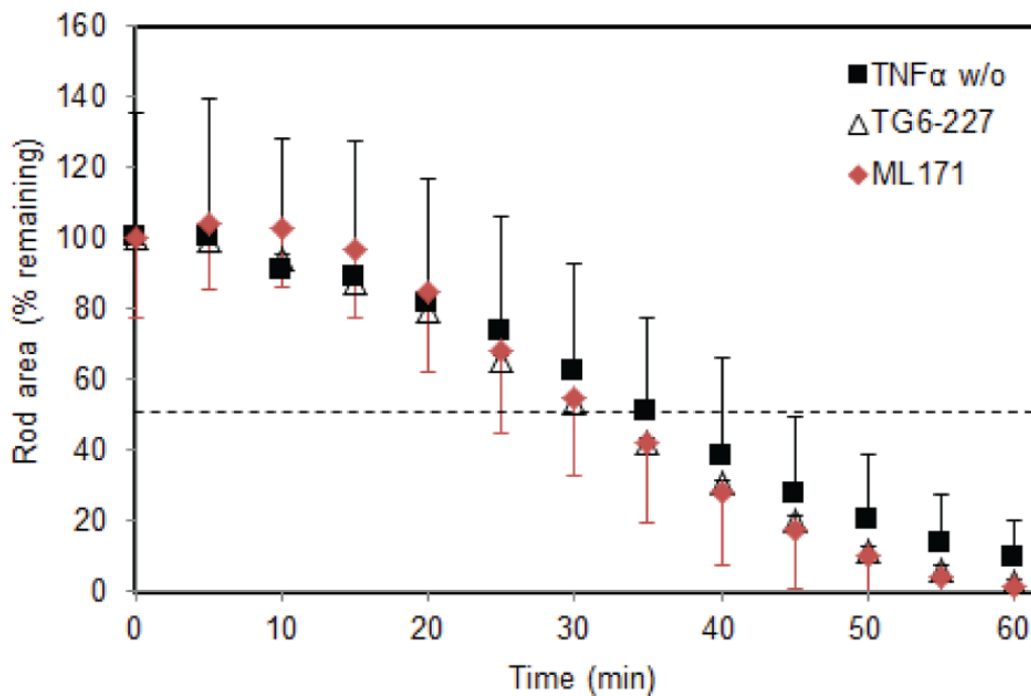


Figure 3.11: Prion-dependent rod reversibility upon NOX inhibition. As shown in *Figure 3.5A*, TG6-227, ML171 and Apocynin reverse rods induced by PrP<sup>C</sup> overexpression quantified after fixing and immunostaining neurons with rods. Here we used live cell imaging of rods visualized using cofilinR21Q-mRFP to follow the time course of rod disappearance, calculated from measurements on 5 rods from 3 independent experiments. Total rod areas were quantified at 5 min intervals for cultures infected with EGFP-PrP<sup>C</sup> that were treated with TG6-227 or ML171. The half-life of PrP<sup>C</sup>-overexpression-induced rods upon addition of NOX inhibitor was 31 min, which is somewhat shorter than that obtained by washing out TNF $\alpha$  (46 min in *Figure 2.5*).

NOX signaling downstream of the prion-dependent pathway is required for rod maintenance.

## Discussion

GPI-linked PrP<sup>C</sup>, a component of lipid raft (LR) domains, serves as a receptor for A $\beta$  (Laurén *et al.*, 2009). We demonstrate that both A $\beta$  and proinflammatory cytokines work via a PrP<sup>C</sup>-dependent mechanism to induce rod formation. The PrP<sup>C</sup>-encoding gene *Prnp* contains polymorphisms at codon 129 (met/val), a known susceptibility factor for Creutzfeldt-Jakob disease (Brown *et al.*, 2000; Ironside & Head, 2004). A comprehensive meta-analysis of M/V polymorphism revealed a modest but significant association with a decreased risk for AD, which is of interest because the polymorphism occurs near the residues (92–110) implicated in binding to A $\beta$  oligomers (Figure 3.1) (He *et al.*, 2013). PrP<sup>C</sup>-dependent signaling pathways have been shown to activate NOX in neurons (Schneider *et al.*, 2003; Pradines *et al.*, 2013). NOX can also be stimulated by TNF $\alpha$  (Barth *et al.*, 2009; 2012) and NOX activity is inversely correlated with cognition (Ansari & Scheff, 2011) as its inhibition proved to have beneficial effects on a variety of incurable central nervous system (CNS) pathologies (Sorce *et al.*, 2012). Using adenovirus to express a redox-sensitive reporter linked to p47<sup>phox</sup>, we show that proinflammatory cytokines and A $\beta$ d/t activate NOX to generate a local increase in ROS, which is confined to a subset of neurites in responding neurons.

The overexpression of PrP<sup>C</sup> alone is sufficient to induce rods without addition of a stressor, such as A $\beta$  or TNF $\alpha$ . Thus, we hypothesize that the clustering of GPI-anchored PrP<sup>C</sup> into membrane microdomains independently recruits the required

oxidizing machinery, including NOX, but is exacerbated by the presence of a stimulus. This idea is reinforced by studies that show the clustering of GPI-linked PrP<sup>C</sup> alone alters the membrane lipid profile and results in density-dependent synaptic damage (Bate & Williams, 2012). GPI-anchored PrP<sup>C</sup> is found in LR microdomains and the size of PrP<sup>C</sup>-containing clusters is enhanced by A $\beta$  (Laurén *et al.*, 2009; Hernandez-Rapp *et al.*, 2014). These domains are distinct areas of the plasma membrane enriched in cholesterol, glycosphingolipid, and sphingomyelin that enhance redox-signaling events by concentrating relevant transmembrane receptors (Brown & London, 1998; Yang & Rizzo, 2007; Zhu *et al.*, 2010). LRs are essential for development, stabilization, and maintenance of synapses (Mauch *et al.*, 2001; Willmann *et al.*, 2006). Cofilin binds to phosphatidylinositol-bis-phosphate (PIP<sub>2</sub>) located in the cytoplasmic leaflet (Yonezawa *et al.*, 1991), which may be concentrated under LR near sites of ROS formation. We suggest that this results in a pool of oxidized, active cofilin available to generate cofilin-actin rods within neurites. The colocalization of the LR and rods can be visualized by staining for both rods and cholera toxin B (CTxB) bound to Gm1 gangliosides, molecules composed of glycosphingolipid and one or more sialic acids, that concentrate in LR (Figure 3.3).

PrP<sup>C</sup> has the capacity to trigger the activation of fyn tyrosine-kinase in neurons through the hairpin-like membrane-inserted protein caveolin-1 (Hernandez-Rapp *et al.*, 2014). NOX-mediated ROS production occurs downstream of fyn activation and may mediate both neural cell adhesion molecule (NCAM)-dependent neurite outgrowth and synaptic dysfunction (Schmitt-Ulms *et al.*, 2001; Schneider *et al.*, 2003; Santuccione *et al.*, 2005; Ittner *et al.*, 2010; Chattopadhyaya *et al.*, 2013). Downstream effects of the

PrP<sup>C</sup>-fyn signaling cascade are amplified by A $\beta$  as it has been shown to enhance both the clustering and crosslinking of PrP<sup>C</sup> at the neuronal cell membrane (Bate & Williams, 2012). A $\beta$ -enhancement of PrP<sup>C</sup>-fyn coupling was tied to the overactivation of the metabotropic mGluR5 as well as the NMDAR (Um *et al.*, 2012; 2013; Hernandez-Rapp *et al.*, 2014). Involvement of the NMDAR suggests that a calcium-dependent mechanism might be involved in synaptic toxicity. Cofilin activation may result from the calcium-dependent activity of calcineurin, which can dephosphorylate and activate SSH to dephosphorylate cofilin (Wang *et al.*, 2005) or through the oxidation of 14-3-3 $\zeta$  to relieve its inhibitory effects on phosphorylated SSH (Kim *et al.*, 2009).

Although several studies have linked A $\beta$  to prion-dependent neurodegenerative mechanisms involving LR microdomains (Malchiodi-Albedi *et al.*, 2010; Rushworth & Hooper, 2011; Bate & Williams, 2012), the results presented here are the first to demonstrate a requirement for cellular prion protein in linking TNF $\alpha$  to the activation of NOX in neurons. We also show that rod formation induced by proinflammatory cytokines, A $\beta$ d/t and overexpressed PrP<sup>C</sup> is reversed by interrupting NOX activation. Likewise, rods reversed by the various inhibitors of NOX demonstrated similar kinetics to the washout of rod-inducing stimuli (Figure 2.6C). This suggests a minimum threshold of ROS that must be exceeded in order to maintain cofilin oxidation and rod stability.

## CHAPTER 4: URSOLIC ACID AND RAP310 INHIBIT AND REVERSE PRION-DEPENDENT ROD FORMATION

### **Introduction**

A large body of evidence demonstrates significant health benefits of nutrient rich fruits and vegetables, including the modulation of inflammation and stress associated with natural aging processes or chronic CNS pathologies (Sun *et al.*, 2008; Spencer, 2009; Szarc vel Szic *et al.*, 2010). Dietary intake of blueberries improved memory and cognition in aging animals and humans (Lau *et al.*, 2005; Krikorian *et al.*, 2010) and attenuated levels of inflammatory cytokines, including TNF $\alpha$  (Sweeney *et al.*, 2002; Shukkit-Hale *et al.*, 2008). Furthermore, Gustafson *et al.* (2012) demonstrated that a nonpolar blueberry fraction prevented TNF $\alpha$ -mediated NOX activation. The fraction had minimal direct antioxidant capacity and was largely devoid of polyphenols, suggesting that the observed effect was a result of interrupting the signaling to activate NOX rather than ROS scavenging (Gustafson *et al.*, 2012). They further demonstrated that exposure to the nonpolar fraction resulted in smaller and discontinuous LR domains, which are otherwise enlarged with TNF $\alpha$  treatment (Lotocki *et al.*, 2004; Vilhardt & Van Deurs, 2004; Li & Gulbins, 2007).

Ursolic acid (UA) is a naturally occurring triterpene that is found in the waxy skin of blueberries as well as cranberries, apples, basil, rosemary, and many other plants (Figure 4.1) (Ikeda *et al.*, 2008). Current research suggests that UA functions in a broad spectrum of therapeutic events, including preventing cancer metastasis (Prasad *et al.*,

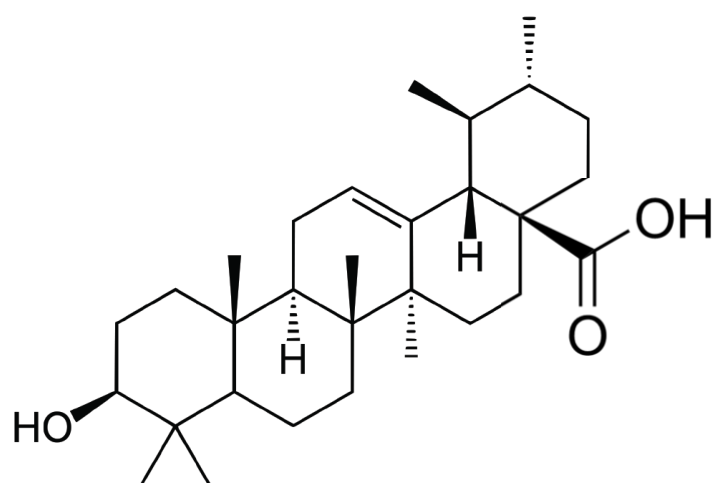


Figure 4.1: UA structure. Ursolic acid (3- $\beta$ -hydroxy-urs-12-ene-28-oic acid) is a naturally occurring pentacyclic triterpenoid. It is found in highest amounts in the protective, wax-like coating of blueberries and apples, and can also be found in basil, cranberries, elderflower, peppermint, rosemary, oregano, thyme, hawthorn and prunes. UA and other various triterpenes have been studied extensively for being starting material for potent bioactive derivatives (i.e. antitumor agents) and for reducing oxidative damage that results from various stimuli, including A $\beta$ .

2012; Zang *et al.*, 2014), promoting muscle repair (Kunkel *et al.*, 2012), and in antimicrobial and biofilm interference (Kim *et al.*, 2011; Zhou *et al.*, 2012). Regarding CNS disorders, UA protects hippocampal neurons against kainite-induced excitotoxicity (Shih *et al.*, 2004), and attenuates cognitive deficits via inflammatory pathways or by restoring mitochondrial function (Wang *et al.*, 2011; Wu *et al.*, 2013; Mortiboys *et al.*, 2013). UA inhibits the deleterious effects of TNF $\alpha$  on cultured neurons (Barth *et al.*, 2012). Thus, we hypothesized that UA would functionally interrupt NOX-dependent rod formation. We also obtained the modified short peptide RAP310 (Rapid Pharmaceuticals, AG). A compound similar to RAP310, D-ala-peptide T-amide (DAPTA), has been shown to remedy the neuroinflammatory cascade in rat models of AD (Rosi *et al.*, 2005) and its parent compound protected aged rats from neuronal loss due to degenerative changes in parietal neocortex (Socci *et al.*, 1996). Here we show that UA and RAP310 prevent the formation of and reverse existing prion-dependent rods in hippocampal neurons.

## **Materials and Methods**

*Neuronal Cell Culture.* Rat E18 cortical and hippocampal neurons were obtained, prepared and maintained as described in Chapter 2.

*Cell Treatments.*

Adenovirus infection. Infections with adenovirus for expressing EGFP-PrP<sup>C</sup> and/or cofilinR21Q-mRFP were done as described previously (Chapter 3).

Rod inducing treatments. Controls and rod-inducing treatments of A $\beta$ d/t, TNF $\alpha$ , IL-1 $\beta$ , IL-6, antimycin A or glutamate were done as described previously (Chapter 3).

### *Reagent Preparation.*

Ursolic acid. Ursolic acid was extracted from wild Alaskan bog blueberries and fractionated by Dr. Thomas Kuhn (University of Alaska-Fairbanks). Prior to experiments concerning the inhibition and reversal of rods, several blueberry fractions (including UA) were tested for their rod-inhibiting abilities. We identified UA and “Fraction 1” (which contained UA) as inhibitors of A $\beta$ -induced rods. UA was stored at 15 mg/ml (-20°C) in dimethyl sulfoxide (DMSO), used at 15  $\mu$ g/ml (32.8  $\mu$ M) and added concurrently with treatments (or up to 2 h for long-term treatments) of glutamate, antimycin A, A $\beta$ d/t, and TNF $\alpha$ . Cell cultures with a UA volume-equivalent DMSO addition served as controls.

RAP310. RAP310 peptide was obtained from Rapid Pharmaceuticals, AG (Hünenberg, Switzerland). It was dissolved in 5.8 ml sterile water, vortexed 30 s, then diluted into 284.2 ml sterile water to give a final concentration of  $1 \times 10^{-6}$  M. Various volume fractions were quick-frozen in liquid nitrogen and stored -80°C or -20°C until used.

*Fixation and Immunostaining, Imaging and Analysis and Statistics* were performed as described in Chapter 2.

## **Results**

*UA inhibits and reverses A $\beta$ d/t- and TNF $\alpha$ -induced rods.* We tested the inhibition of rods by various fractions of extracts prepared from wild Alaskan bog blueberries, one of which included UA as the major component (data not shown). Preliminary data suggested that the UA-containing fraction and UA alone both prevented A $\beta$ d/t-induced rod formation. In dissociated hippocampal neurons treated 24 h with A $\beta$ d/t and TNF $\alpha$  and cultures were fixed in the presence of UA, we found a dose-dependent inhibition of

rod formation with maximal inhibition at 15 mg/ml UA (Figure 4.2A). UA (15 mg/ml) was added to neurons treated ~24 h with TNF $\alpha$  at time intervals up to 2 h. Rods were visualized by immunostaining and quantified both in terms of the percent of neurons with rods and the number rod index (rods per cell body). Both the percent of neurons with rods (Figure 4.2B) and rod index (Figure 4.2C) were reduced to untreated control levels after ~1 h.

The shortening of rods precedes their complete dissolution and thus, shorter, “reversing” rods are still scored as a positive rod in fixed neurons. We therefore demonstrated that increasing times of UA treatment resulted in a percent of rods with a shorter defined pixel length (Figure 4.2D).

*RAP310 inhibits and reverses A $\beta$ d/t- and TNF $\alpha$ -induced rods.* RAP310 was shown to modulate the inflammatory response in rat AD models (Rosi *et al.*, 2005) and thus we hypothesized that it might effect rod formation. An approximate concentration range to test ( $10^{-14}$ - $10^{-8}$  M) was recommended by Rapid Pharmaceuticals based on previous data. RAP310 demonstrated a dose-dependent inhibition of rod formation when added concurrently with A $\beta$ d/t for 24 h, with a full inhibitory response at approximately  $10^{-12}$  M (Figure 4.3A). RAP310 ( $10^{-10}$  M) reversed rod formation by A $\beta$ d/t, but not by glutamate (Figure 4.3B), suggesting that RAP310 works by disrupting the prion-dependent pathway for NOX activation.

*Reversal of A $\beta$ d/t- and TNF $\alpha$ -stimulated ROS production by UA and RAP310.* ROS production can be measured within neurites of neurons infected with a redox-

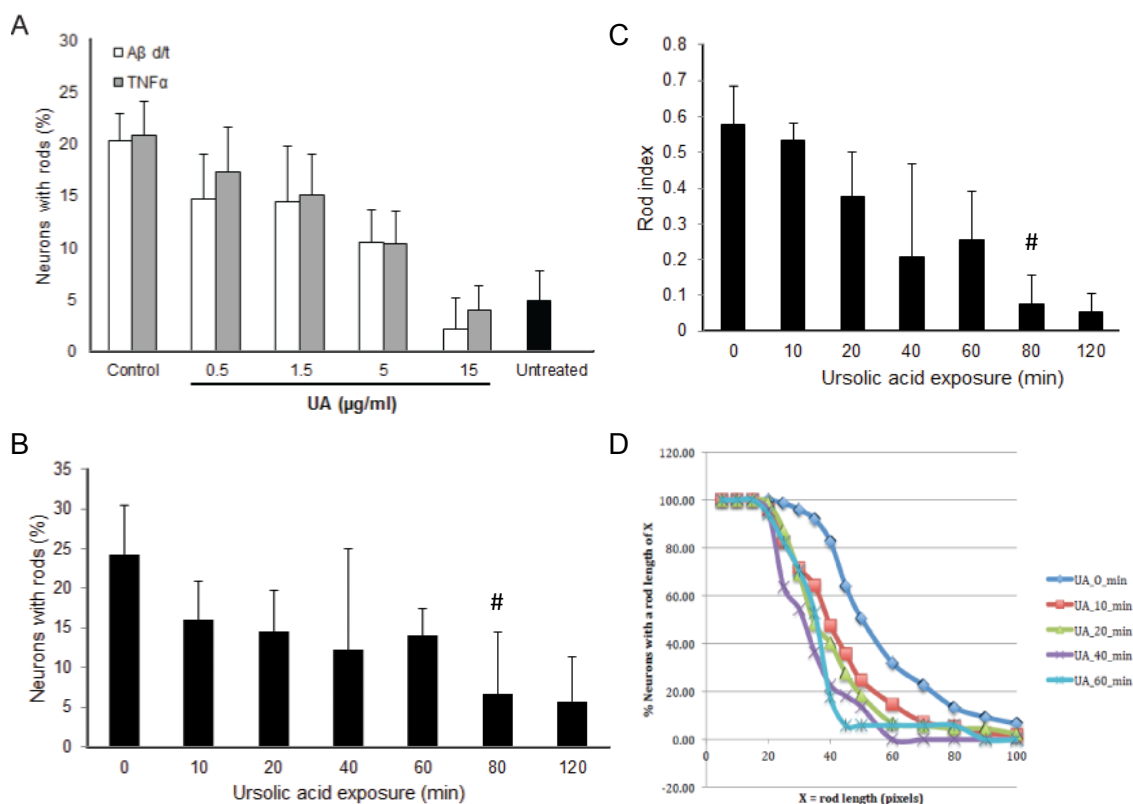


Figure 4.2: UA inhibits and reverses Aβd/t- and TNFα-induced rods. (A) Hippocampal neurons were treated 24 h with Aβd/t and TNFα in the presence of a spectrum of UA concentrations before fixing, immunostaining and quantifying the percent of cells with rods. UA prevented rod formation in a dose-dependent manner with a maximal response at 15 mg/ml, thus this concentration was used for subsequent experiments. The percent of neurons with TNFα-induced rods (B) and the approximate number of rods per cell body (C) both decrease over a time course of UA treatment. Rods reverse to a significant (# p<0.001) level after ~80 min. (D) The shortening of cofilin-containing rods was analyzed over a time course of UA exposure for neurons treated 24 h with TNFα. Rods became shorter over time of exposure to UA.

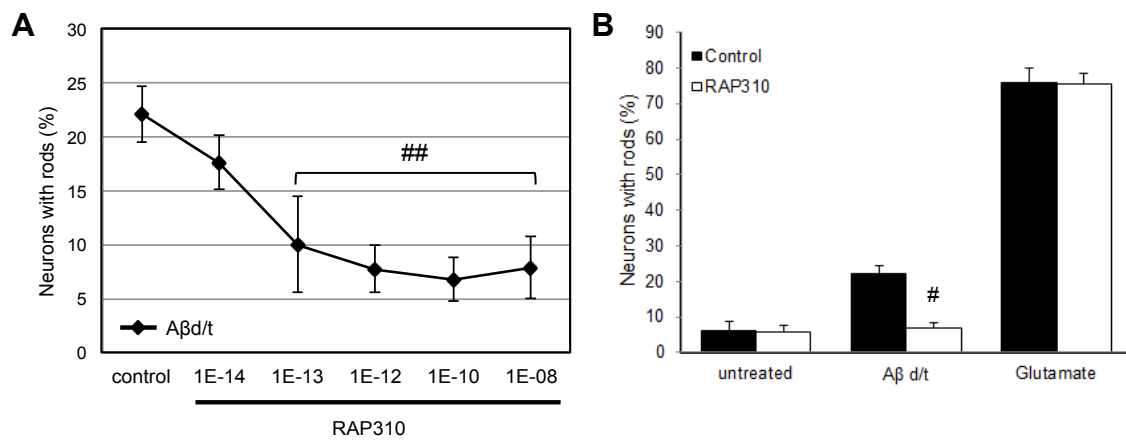


Figure 4.3: RAP310 inhibits rods induced by Aβd/t and TNFα, but not by glutamate. (A) Cells were treated for 24 h with Aβd/t and various dilutions of RAP310. Similar to UA, RAP310 demonstrated a significant (## p<0.005) dose-dependent inhibition beginning at 10<sup>-13</sup> M with a maximal response at 10<sup>-10</sup> M. A 10<sup>-10</sup> M concentration was used for subsequent studies. (B) RAP310 reversed rods formed by Aβd/t (# p<0.001) but not by glutamate.

sensitive p47-roGFP reporter for NOX activity after exposure to A $\beta$ d/t (~250 pM) or TNF $\alpha$  (100 ng/ml) (Figure 4.4A). Both UA (15 mg/ml) (Figure 4.4B) and RAP310 (10<sup>-10</sup> M) (Figure 4.4C) reduced roGFP fluorescence back to control levels over about a 15 min period when added after 30 min of A $\beta$ d/t or TNF $\alpha$  treatment.

*Reversal of prion-dependent rods by UA and RAP310.* To determine if UA and RAP310 inhibit rods induced by PrP<sup>C</sup> overexpression, neurons were infected on day 2 with 100 MOI EGFP-PrP<sup>C</sup> adenovirus for 60 h and UA or RAP310 was added for 2 h prior to fixation. Both compounds significantly (p<0.001) reversed rods (stained with Alexa 594 secondary antibody) in fixed cultures (Figure 4.5) at the same concentrations that they were used to reverse ROS production.

## **Discussion**

A vast field of research is dedicated to identifying a nutritional basis for decreasing oxidative stress markers in various neurodegenerative disorders (Gillette-Guyonnet *et al.*, 2013; Bernard *et al.*, 2014; Seidl *et al.*, 2014). Since oxidative stress is a marker for mild or early cognitive impairment (Keller *et al.*, 2005), various nutraceutical compounds in fruits and vegetables may modulate production of ROS that contributes to acute and chronic neurodegeneration. We show here that UA, a naturally occurring triterpenoid, reverses rod formation by A $\beta$ d/t and proinflammatory cytokines. UA was shown to inhibit A $\beta$  binding to microglial receptor CD36, resulting in reduced proinflammatory cytokine production and neurotoxic ROS (Wilkinson *et al.*, 2011). In addition, primary hippocampal neurons exposed to blueberry extracts showed

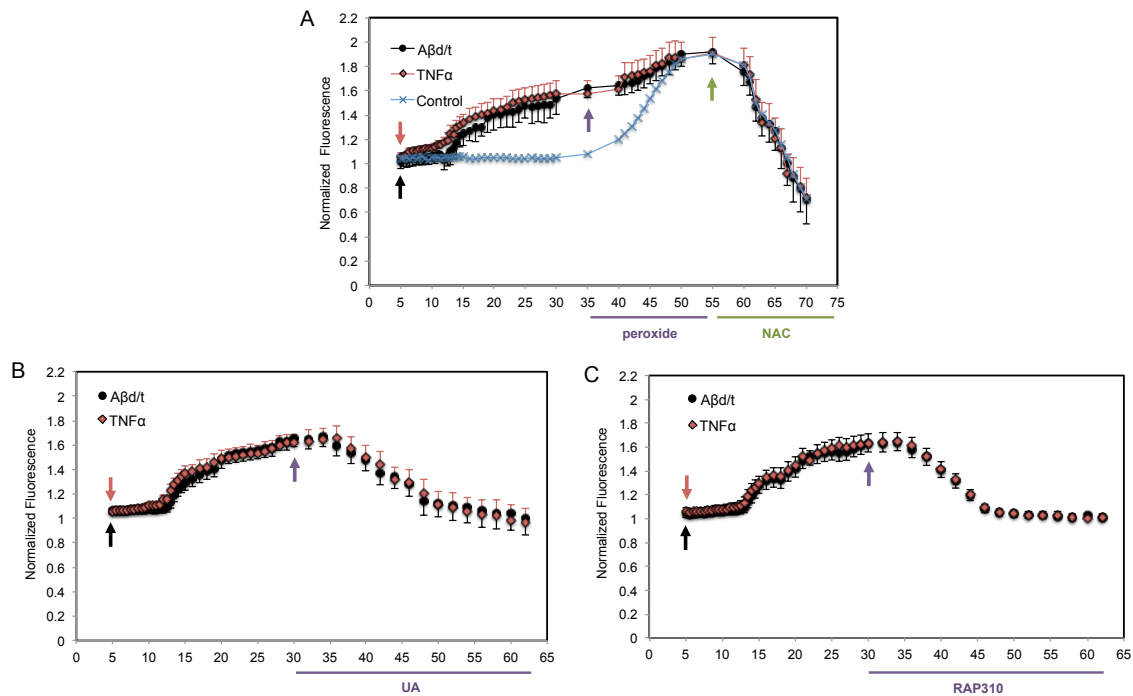


Figure 4.4: UA and RAP310 reverse Aβd/t- and TNFα-induced ROS production. (A) As shown in Figure 3.10, fluorescence increased in neurites of neurons infected 36 h with a redox-sensitive p47-roGFP NOX activity reporter after treatment with Aβd/t and TNFα. (B) Ursolic acid (UA) (15 mg/ml) and (C) RAP310 ( $10^{-10}$  M) reversed both Aβd/t- and TNFα-induced ROS production to the normalized untreated level when added after 30 min.

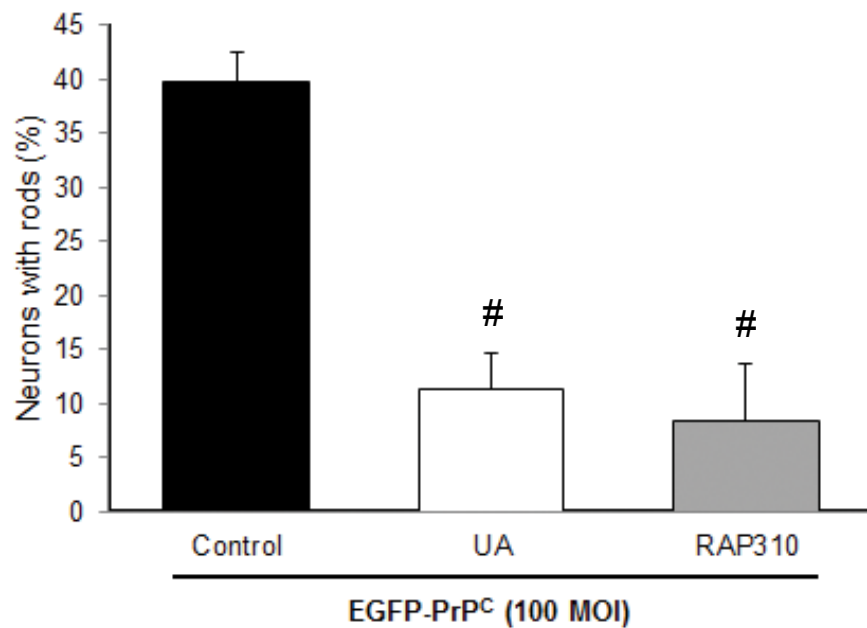


Figure 4.5: RAP310 and UA reverse rods induced by PrP<sup>C</sup> overexpression. Cells were infected 60 h with 100 MOI of EGFP-PrP<sup>C</sup> adenovirus, and then UA (15 mg/ml) or RAP310 (10<sup>-10</sup> M) was added for 1 h prior to fixing, immunostaining, and scoring for the percent of neurons with rods. Both compounds significantly (# p<0.001) reversed rods similarly to the reversal of rods after NOX inhibition (*Figure 3.5A*).

improved calcium recovery and cell viability while reducing free radical levels in response to A $\beta$  (Joseph *et al.*, 2007). UA also improves cognitive deficits and attenuates oxidative damage and neuroinflammation due to a D-galactose-induced inflammatory response in mouse brain (Lu *et al.*, 2007; 2010)

The function of UA in reducing neurotoxic ROS levels may be explained at the level of lipid membrane properties. LR domains are enriched in sphingomyelin (Brown & London, 1998; Yang & Rizzo, 2007), an abundant plasma membrane lipid. TNF $\alpha$  stimulates sphingomyelinase, which generates ceramide by hydrolysis of sphingomyelin. The TNF $\alpha$ -induced production of ceramide and subsequent NOX-dependent ROS generation in neuroblastoma cells (Barth *et al.*, 2012) is inhibited when cells are pretreated with nonpolar blueberry fractions (Gustafson *et al.*, 2007). The bioactive lipid ceramide, along with cholesterol, is a primary contributor to the overall mechanical stability of the lipid bilayer of LR domains (Castro *et al.*, 2014). Thus, UA might reverse rod formation by interrupting membrane lipid modifications that enhance the coalescence of large, PrP<sup>C</sup>-containing LR domains.

Oxidative stress and overproduction of proinflammatory factors play a significant role in cognitive impairment as a result HIV-1 infection (Persidsky *et al.*, 2011) that manifests as HIV-associated dementia (Zhou & Saksena, 2013). A related compound to RAP310, DAPTA, is a peptide that blocks CCR5 chemokine receptors for the HIV viral entry glycoprotein gp120 (Ruff *et al.*, 2003). Binding of gp120 to LR-colocalized CCR5 or CXCR4 (CD4) on host T-helper cells induces a cascade of conformational changes that leads to fusion with the host cell membrane (Popik *et al.*, 2002). Coalescence of LR microdomains is primarily required for gp120 binding and ultimately HIV entry (Mañes *et*

*al.*, 2000; Lee *et al.*, 2009; Kamiyama *et al.*, 2009). In addition, we have preliminary evidence that suggests gp120 induces both ROS generation and rod formation in hippocampal neurons. Taken together, these data support our idea of an enlarged membrane signaling platform for cofilin oxidation that leads to rod formation. Although only speculation at this time, RAP310 may work directly in binding to receptors that can disrupt their coalescence into these signaling platforms, whereas UA might work to disrupt the lipid matrix that supports these interactions.

Our results suggest that preventing the generation of ROS may be just as important as its sequestration by redox agents, such as antioxidants. We show here that UA and RAP310 inhibit rod formation and reverse existing rod structures induced by A $\beta$  and TNF $\alpha$  in dissociated hippocampal neurons, but not those produced by excitotoxic glutamate. This reinforces our demonstration of two different mechanisms for rod induction, one that requires the prion-dependent activation of NOX, and one that is altogether NOX-independent.

## CHAPTER 5: CONCLUSIONS AND FUTURE DIRECTIONS

We have shown that A $\beta$ d/t and proinflammatory cytokines utilize a cellular prion protein (PrP<sup>C</sup>)-dependent signaling pathway to activate NADPH oxidase (NOX). At these enlarged membrane microdomains, signaling exceeds a critical threshold of reactive oxygen species (ROS) to maintain an activated and oxidized pool of cofilin that forms cofilin-actin rods (Figure 1.6). We and others have previously shown that rods interrupt vesicular transport that is vital for synaptic function (Minamide *et al.*, 2000; Maloney *et al.*, 2005; Cichon *et al.*, 2012; Mi *et al.*, 2013).

Neurofibrillary tangles (NFT) are a pathogenic marker of both repetitive traumatic brain injury-induced chronic traumatic encephalopathy (CTE) (McKee *et al.*, 2014) and Alzheimer disease (AD) (Hernández & Avila, 2007), connecting neuroinflammatory and neurodegenerative disorders. PrP<sup>C</sup> has been linked to the activation of fyn tyrosine-kinase in neurons via the hairpin-like membrane-inserted protein caveolin-1 (Hernandez-Rapp *et al.*, 2014). Identifying caveolin-1 with PrP<sup>C</sup> at sites of rod formation and studying both rod inhibition and reversal dynamics using fyn inhibitors are future experiments that will help to clarify these the relationships between these proteins in rod signaling.

In addition to NOX activation, the PrP<sup>C</sup>-fyn pathway has been shown to promote tau hyperphosphorylation in response to A $\beta$  oligomers (Larson *et al.*, 2012). Therefore, it is possible that one mechanism for tau hyperphosphorylation is tied to (but not required for) rod formation. Once phosphorylated, tau is prevented from binding

microtubules and can assemble into paired helical filaments that deposit as neuropil threads or into larger aggregated NFTs (Figure 1.2). Given that NFTs and amyloid plaques do not always correlate with cognitive status (Hernández & Avila, 2007; Scheff *et al.*, 2014), it is possible that cofilin-actin rods account for synaptic dysfunction in some cohort of AD subjects and maybe in early stages of cognitive impairment. Current experiments quantifying rods and tau pathology in different regions of post-mortem human brain tissue obtained from subjects at different stages of cognitive decline will shed some light in this area.

We demonstrate here that ursolic acid (UA) and RAP310 inhibit and reverse rod formation possibly by disrupting the coalescence of lipid raft (LR) domains and preventing the recruitment of oxidizing machinery. Further investigation is required to characterize this dynamic process by tying the dispersion of PrP<sup>C</sup>-containing, CTxB-stained LRs to the dissolution of rods in real time. Studies of UA and RAP310 reversal of A $\beta$ d/t- and TNF $\alpha$ -induced ROS generation using the p47-roGFP adenovirus are currently underway.

The vast majority of Alzheimer disease (AD) cases are considered sporadic in incidence and multifactorial in cause, making treatment of the disease at an early stage challenging (Pruta R *et al.*, 2013). Thus, being able to bridge multiple disease initiating mechanisms, such as A $\beta$  overproduction or neuroinflammation triggered by proinflammatory cytokines, into a common pathway for synapse loss provides a valuable focus for therapeutic agents. The formation of cofilin-actin rods provides such a target.

## REFERENCES

- Abe H, Ohshima S, Obinata T (1989) A cofilin-like protein is involved in the regulation of actin assembly in developing skeletal muscle. *J Biochem* 106:696-702.
- Aguzzi A, Heikenwalder M (2006) Pathogenesis of prion diseases: current status and future outlook. *Nat Rev Microbiol* 4:765-75.
- Altenhofer S, Radermacher KA, Kleikers PW, Wingler K, Schimdt HH (2014) Evolution of NADPH oxidase inhibitors: selectivity and mechanisms for target engagement. *Antioxid Redox Signal* (Epub ahead of print).
- Alzheimer's Association. 2014 Alzheimer's Disease Facts and Figures, *Alzheimer's & Dementia* 10:6-52.
- Amor S, Puentes F, Baker D, van der Valk P (2010) Inflammation in neurodegenerative diseases. *Immunology* 129:154-69.
- Amor S, Peferoen LA, Vogel DY, Breur M, van der Valk P, Baker D, van Noort JM (2014) Inflammation in neurodegenerative diseases – an update. *Immunology* 142:151-66.
- Andrianantoandro E, Pollard TD (2006) Mechanism of actin filament turnover by severing and nucleation at different concentrations of ADF/Cofilin. *Mol Cell* 24:13-23.
- Ansari MA, Scheff SW (2011) NADPH-oxidase activation and cognition in Alzheimer disease progression. *Free Radic Biol Med* 51:171-8.
- Atwood CS, Perry G, Zeng H, Kato Y, Jones WD, Ling KQ, Huang X, Moir RD,

- Wang D, Sayre LM, Smith MA, Chen SG, Bush AI (2004) Copper mediates dityrosine cross-linking of Alzheimer's amyloid-beta. *Biochemistry* 43:560-8.
- Bagyinszky E, Youn YC, An SS, Kim S (2014) The genetics of Alzheimer's disease. *Clin Interv Aging* 9:535-51.
- Bamburg JR, Bernstein BW (2010) Roles of ADF/cofilin in actin polymerization and beyond. *F1000 Biol Rep*: 2:62.
- Bamburg JR, Bernstein BW, Davis RC, Flynn KC, Goldsbury C, Jensen JR, Maloney MT, Marsden IT, Minamide LS, Pak CW, Shaw AE, Whiteman I, Wiggan O (2010) ADF/Cofilin-actin rods in neurodegenerative diseases. *Curr Alzheimer Res* 7:241-50.
- Bamburg JR, Bloom GS (2009) Cytoskeletal pathologies of Alzheimer disease. *Cell Motil Cytoskeleton* 66:635-49.
- Barry AE, Klyubin I, McDonald JM, Mably AJ, Farrell MA, Scott M, Walsh DM, Rowan MJ (2011) Alzheimer's disease brain-derived amyloid- $\beta$ -mediated inhibition of LTP in vivo is prevented by immunotargeting cellular prion protein. *J Neurosci* 31:7259-63.
- Barth BM, Gustafson SJ, Hankins JL, Kaiser JM, Haakenson JK, Kester M, Kuhn TB (2012) Ceramide kinase regulates TNF $\alpha$ -stimulated NADPH oxidase activity and eicosanoid biosynthesis in neuroblastoma cells. *Cell Signal* 24:1126-33.
- Barth BM, Stewart-Smeets S, Kuhn TB (2009) Proinflammatory cytokines provoke oxidative damage to actin in neuronal cells mediated by Rac1 and NADPH oxidase. *Mol Cell Neurosci* 41(2):274-85.
- Bate C, Williams A (2011) Amyloid- $\beta$ -induced synapse damage is mediated via

- cross-linkage of cellular prion protein. *J Biol Chem* 286:37955-63.
- Bate C, Williams A (2012) Neurodegeneration induced by clustering of sialylated glycosylphosphatidylinositols of prion proteins. *J Biol Chem* 287:7935-44.
- Bedard K, Krause KH (2007) The NOX family of ROS-generating NADPH oxidases: physiology and pathophysiology. *Physiol Rev* 87:245-313.
- Bernard ND, Bush AI, Ceccarelli A, Cooper J, de Jager CA, Erickson KI, Fraser G, Kesler S, Levin SM, Lucey B, *et al.* (2014) Dietary and lifestyle guidelines for the prevention of Alzheimer's disease. *Neurobiol Aging* S0197-4580:00348-0.
- Bernstein BW, Chen H, Boyle JA, Bamberg JR (2006) Formation of actin-ADF/cofilin rods transiently retards decline of mitochondrial potential and ATP in stressed neurons. *Am J Physiol Cell Physiol* 291:C828-39.
- Bernstein BW, Shaw AE, Minamide LS, Pak CW, Bamberg JR (2012) Incorporation of cofilin into rods depends on disulfide intermolecular bonds: implications for actin regulation and neurodegenerative disease. *J Neurosci* 19:6670-81.
- Bertram L, Tanzi RE (2004) The current status of Alzheimer's disease genetics: what do we tell the patients? *Pharmacol Res* 50:385-96.
- Braak H, Braak E (1995) Staging of Alzheimer's disease-related neurofibrillary changes. *Neurobiol Aging* 16:271-8.
- Breunig JJ, Guillot-Sestier MV, Town T (2013) Brain injury, neuroinflammation and Alzheimer's disease. *Front Agin Neurosci* 5:26.
- Briones TL, Woods J, Rogozinska M (2013) Decreased neuroinflammation and

- increased brain energy homeostasis following environmental enrichment after mild traumatic brain injury is associated with improvement in cognitive function. *Acta Neuropathol Commun* 1:57.
- Brown DA, London E (1998) Function of lipid rafts in biological membranes. *Annu Rev Cell Dev Biol* 14:111-36.
- Brown P, Preece M, Brandel JP, Sato T, McShane L, Zerr I, Fletcher A, Will RG, Pocchiari M, Cashman NR (2000) Iatrogenic Creutzfeldt-Jakob disease at the millennium. *Neurology* 55:1075-81.
- Cacquevel M, Lebeurrier N, Chéenne S, Vivien D (2004) Cytokines in neuroinflammation and Alzheimer's disease. *Curr Drug Targets* 5:529-34.
- Campus SB, Ashworth SL, Wean S, Hosford M, Sandoval RM, Hallett MA, Atkinson SJ, Molitoris BA (2009) Cytokine-induced F-actin reorganization in endothelial cells involves RhoA activation. *Am J Physiol Renal Physiol* 296:F487-95.
- Castro BM, Prieto M, Silva LC (2014) Ceramide: A simple sphingolipid with unique biophysical properties . *Prog Lipid Res* 54:53-67.
- Chattopadhyaya B, Baho E, Huang ZJ, Schachner M, Di Cristo G (2013) Neural cell adhesion molecule-mediated Fyn activation promotes GABAergic synapse maturation in postnatal mouse cortex. *J Neurosci* 33:5957-68.
- Chung E, Ji Y, Sun Y, Kascsak RJ, Kascsak RB, Mehta PD, Strittmatter SM, Wisniewski T (2010) Anti-PrPC monoclonal antibody infusion as a novel treatment for cognitive deficits in an Alzheimer's disease model mouse. *BMC Neurosci* 11:130.

- Cichon J, Sun C, Chen B, Jiang M, Chen XA, Sun Y, Wang Y, Chen G (2012) Cofilin aggregation blocks intracellular trafficking and induces synaptic loss in hippocampal neurons. *J Biol Chem* 287:3919-29.
- Cleary JP, Walsh DM, Hofmeister JJ, Shankar GM, Kuskowski MA, Selkoe DJ, Ashe KH (2005) Natural oligomers of the amyloid-beta protein specifically disrupt cognitive function. *Nat Neurosci* 8:79-84.
- Cooper JA, Schafer DA (2000) Control of actin assembly and disassembly at filament ends. *Curr Biol* 12:97-103.
- Davis RC, Maloney MT, Minamide LS, Flynn KC, Stonebraker MA, Bamburg JR (2009) Mapping cofilin-actin rods in stressed hippocampal slices and the role of cdc42 in amyloid  $\beta$ -induced rods. *J Alz Dis* 18:35-50.
- Davis RC, Marsden IT, Maloney MT, Minamide LS, Podlisny M, Selkoe D, Bamburg JR (2011) Amyloid beta dimers/trimers potently induce cofilin-actin rods that are inhibited by maintaining cofilin-phosphorylation. *Mol Neurodegen* 6:1-17.
- Eehalt R, Keller P, Haass C, Thiele C, Simons K (2003) Amyloidogenic processing of the Alzheimer beta-amyloid precursor protein depends on lipid rafts. *J Cell Bio* 160:113-23.
- Ermonval M, Mouillet-Richard S, Codongo P, Kellermann O, Botti J (2003) Evolving views in prion glycosylation: functional and pathological implications. *Biochimie* 85:33-45.
- Ferreira AP, Rodrigues FS, Della-Pace ID, Mota BC, Oliveira SM, Velho Gewehr CD, Bobinski F, de Oliveira CA, Brum JS, Oliveira MS, *et al.* (2013) The effect of NADPH-oxidase inhibitor apocynin on cognitive impairment induced by moderate

- lateral fluid percussion injury: Role of inflammatory and oxidative brain damage. *Neurochem Int* 63:583-93.
- Feuerstein GZ, Liu T, Barone FC (1994) Cytokines, inflammation, and brain injury: role of tumor necrosis factor- $\alpha$ . *Cerebrovasc Brain Met Rev* 6:341-60.
- Gillette-Guyonnet S, Secher M, Vellas B (2013) Nutrition and neurodegeneration: epidemiological evidence and challenges for future research. *Br J Clin Pharmacol* 75:738-55.
- Griffin WS, Barger SW (2010) Neuroinflammatory cytokines – the common thread in Alzheimer’s pathogenesis. *US Neurol* 6:19-27.
- Groemping Y, Rittinger K (2005) Activation and assembly of the NADPH oxidase: a structural perspective. *Biochem J* 386:401-16.
- Gu J, Lee CW, Fan Y, Komlos D, Tang X, Sun C, Yu K, Hartzell HC, Chen G, Bamberg JR, Zheng JQ (2010) ADF/cofilin-mediated actin dynamics regulate AMPA receptor trafficking during synaptic plasticity. *Nat Neurosci* 13:1208-15.
- Gustafson SJ, Barth BM, McGill CM, Clausen TP, Kuhn TB (2007) Wild Alaskan blueberry extracts inhibit a magnesium-dependent neutral sphingomyelinase activity in neurons exposed to TNF $\alpha$ . *Curr Topics Nutraceut Res* 5:183-8.
- Gustafson SJ, Dunlap KL, McGill CM, Kuhn TB (2012) A nonpolar blueberry fraction blunts NADPH oxidase activation in neuronal cells exposed to tumor necrosis factor- $\alpha$ . *Oxid Med Cell Longev* 2012:768101
- Haigh CL, Edwards K, Brown DR (2005) Copper binding is the governing determinant of prion protein turnover. *Mol Cell Neurosci* 30:186-96.
- Hamos JE, DeGennaro LF, Drachman DA (1989) Synaptic loss in Alzheimer’s

- disease and other dementias. *Neurology* 39:355-61.
- He J, Li X, Yang J, Huang J, Fu X, Zhang Y, Fan H (2013) The association between the methionine/valine (M/V) polymorphism (rs1799990) in the PRNP gene and the risk of Alzheimer disease: an update by meta-analysis. *J Neurol Sci* 326:89-95.
- He TC Zhou S, da Costa LT, Yu J, Kinzler KW, Vogelstein B (1998) A simplified system for generating recombinant adenoviruses. *Proc Natl Acad Sci USA* 95:2509-14.
- Hernández F, Avila J (2007) Tauopathies. *Cell Mol Life Sci* 64:2219-33.
- Hernandez-Rapp J, Martin-Lannerée S, Hirsch TZ, Launay JM, Mouillet-Richard S (2014) Hijacking PrP<sup>C</sup>-dependent signal transduction: when prions impair A $\beta$  clearance. *Front Aging Neurosci* 6:00025-30.
- Hordijk PL (2006) Regulation of the NADPH oxidases: the role of Rac proteins. *Circ Res* 98:453-62.
- Huang TY, DerMardirossian C, Bokoch GM (2006) Cofilin phosphatases and regulation of actin dynamics. *Curr Opin Cell Biol* 18:26-31.
- Ikeda Y, Murakami A, Ohigashi H (2008) Ursolic acid: an anti- and pro-inflammatory triterpenoid. *Mol Nutr Food Res* 52:26-42.
- Ironside JW, Head MW (2004) Variant Creutzfeldt-Jakob disease: risk of transmission by blood and blood products. *Haemophilia* 4:64-9.
- Ittner LM, Ke YD, Delerue F, Bi M, Gladbach A, van Eersel J, Wölfing H, Chieng BC, Christie MJ, Napier IA, Eckert A, Staufenbiel H, Hardeman E, Götz J (2010) Dendritic function of tau mediates amyloid-beta toxicity in Alzheimer's disease

mouse models. *Cell* 142:387-97.

Jonsson T, Atwal JK, Steinberg S, Snaedal J, Jonsson PV, Bjornsson S, Stefansson H, Sulem P, Gudbjartsson D, Maloney J, *et al.* (2012) A mutation in APP protects against Alzheimer's disease and age-related cognitive decline. *Nature* 488:96-9.

Joseph JA, Carey A, Brewer GJ, Lau FC, Fisher DR (2007) Dopamine and Abeta-induced stress signaling and decrements in Ca<sup>2+</sup> buffering in primary neonatal hippocampal cells are antagonized by blueberry extract. *J Alzheimers Dis* 11:433-46.

Kamiyama H, Yoshii H, Tanaka Y, Sato H, Yamamoto N, Kubo Y (2009) Raft localization of CXCR4 is primarily required for X4-tropic immunodeficiency virus type 1 infection. *Virology* 386:23-31.

Keller JN, Schmitt FA, Scheff SW, Ding Q, Chen Q, Butterfield DA, Markesbery WR (2005) Evidence of increased oxidative damage in subjects with mild cognitive impairment. *Neurology* 64:1152-6.

Kim E, Sy-Cordero A, Graf TN, Brantley SJ, Paine MF, Oberlies NH (2011) Isolation and identification of intestinal CYP3A inhibitors from cranberry (*Vaccinium macrocarpon*) using human intestinal microsomes. *Planta Med* 77:265-70.

Kim JS, Huang TY, Bokoch GM (2009) Reactive oxygen species regulate a slingshot-cofilin activation pathway. *Mol Biol Cell* 20:2650-60.

Klamt F, Zdanov S, Levine RL, Pariser A, Zhang Y, Zhang B, Yu LR, Veenstra

- TD, Shacter E (2009) Oxidant-induced apoptosis is mediated by oxidation of the actin-regulatory protein cofilin. *Nat Cell Bio* 11:1241-6.
- Krause KH, Lambeth D, Krönke M (2012) NOX enzymes as drug targets. *Cell Mol Life Sci* 69:2279-82.
- Krikorian R, Shidler MD, Nash TA (2010) Blueberry supplementation improves memory in older adults. *J Agric Food Chem* 58:3996-4000.
- Kunkel SD, Elmore CJ, Bongers KS, Ebert SM, Fox DK, Dyle MC, Bullard SA, Adams CM (2012) Ursolic acid increases skeletal muscle and brown fat and decreases diet-induced obesity, glucose intolerance and fatty liver disease. *PLoS One* 7:e39332.
- Lambeth JD (2004) NOX enzymes and the biology of reactive oxygen. *Nat Rev Immunol* 4:181-9.
- Larson M, Sherman MA, Amar F, Nuvolone M, Scheinder JA, Bennett DA, Aguzzi A, Lesné SE (2012) The complex PrP(c)-Fyn couples human oligomeric A $\beta$  with pathological tau changes in Alzheimer's disease. *J Neurosci* 32:16857-71.
- Lau FC, Shukitt-Hale B, Joseph JA (2005) The beneficial effects of fruit polyphenols on brain aging. *Neurobiol Aging* 26:S128-32.
- Laurén J, Gimbel DA, Nygaard HB, Gilbert JW, Strittmatter SM (2009) Cellular prion protein mediates impairment of synaptic plasticity by amyloid-beta oligomers. *Nature* 457:1128-32.
- Lee DY, Lin X, Paskaleva EE, Liu Y, Puttamadappa SS, Thornber C, Drake JR,

- Habulin M, Shekhtman A, Canki M (2009) Palmitic acid is a novel CD4 fusion inhibitor that blocks HIV entry and infection. *AIDS Res Hum Retroviruses* 25:1231-41.
- Li PL, Gulbins E (2007) Lipid rafts and redox signaling *Antiox & Redox* 9:1411-5.
- Lin Y, Wen L (2013) Inflammatory response following diffuse axonal injury. *Int J Med Sci* 10:515-21.
- Liu L, Chan C (2014) The role of inflammasome in Alzheimer's disease. *Ageing Res Rev* 15:6-15.
- Longhi L, Perego C, Ortolano F, Aresi S, Fumagalli S, Zanier ER, Stocchetti N, De Simoni MG (2013) Tumor necrosis factor in traumatic brain injury: effects of genetic deletion of p55 or p75 receptor. *J Cereb Blood Flow Metab* 33:1182-9.
- Lotocki G, Alonso OF, Dietrich WD, Keane RW (2004) Tumor necrosis factor receptor 1 and its signaling intermediates are recruited to lipid rafts in the traumatized brain. *J Neurosci* 24:11010-6.
- Luchsinger JA, Mayeux R (2004) Dietary factors and Alzheimer's disease. *Lancet Neurol* 3:579-87.
- Lu J, Wu DM, Zheng YL, Hu B, Zhang ZF, Ye Q, Liu CM, Shan Q, Wang YJ (2010) Ursolic acid attenuates D-galactose-induced inflammatory response in mouse prefrontal cortex through inhibiting AGEs/RAGE/NF- $\kappa$ B pathway activation. *Cereb Cortex* 20:2540-8.
- Lu J, Zheng YL, Wu DM, Luo L, Sun DX, Shan Q (2007) Ursolic acid ameliorates cognition deficits and attenuates oxidative damage in the brain of senescent mice induced by D-galactose. *Biochem Pharmacol* 74:1078-90.

- Malchiodi-Albedi F, Contruscieri V, Raggi C, Fecchi K, Rainaldi G, Paradisi S, Matteucci A, Santini MT, Sargiacomo M, Frank C, *et al.* (2010) Lipid raft disruption protects mature neurons against amyloid oligomer toxicity. *Biochim Biophys Acta* 1802:406-15.
- Maloney MT, Bamburg JR (2007) Cofilin-mediated neurodegeneration in Alzheimer's disease and other amyloidopathies. *Mol Neurobiol* 35:21-44.
- Maloney MT, Minamide LS, Kinley AW, Boyle JA, Bamburg JR (2005) Beta-secretase-cleaved amyloid precursor protein accumulates at actin inclusions induced in neurons by stress or amyloid beta: a feedforward mechanism for Alzheimer's disease. *J Neurosci* 25:11313-21.
- Mañes S, del Real G, Lacalle RA, Lucas P, Gómez-Moutón C, Sánchez-Palomino S, Delgado R, Alcamí J, Mira E, Martínez-A C (2000) Membrane raft microdomains mediate lateral assemblies required for HIV-1 infection. *EMBO Rep* 1:190-6.
- Masters CL, Selkoe DJ (2012) Biochemistry of amyloid  $\beta$ -protein and amyloid deposits in Alzheimer disease. *Col Spring Harb Perspect Med* 2:a006262.
- Mauch DH, Nägler K, Schumacher S, Göritz C, Müller EC, Otto A, Pfrieger FW (2001) CNS synaptogenesis promoted by glia-derived cholesterol. *Science* 294:1354-7.
- McDonald JM, Cairns NJ, Taylor-Reinwald L, Holtzman D, Walsh DM (2012) The levels of water-soluble and triton-soluble A $\beta$  are increased in Alzheimer's disease brain. *Brain Res* 1450:138-47.
- McDonald JM, Savva GM, Brayne C, Welzel AT, Forster G, Shankar GM, Selkoe

- DJ, Ince PG, Walsh DM (2010) The presence of sodium dodecyl sulphate-stable Aβ dimers is strongly associated with Alzheimer-type dementia. *Brain* 133:1328-41.
- McKee AC, Daneshvar DH, Alvarez VE, Stein TD (2014) The neuropathology of sport. *Acta Neuropathol* 127:29-51.
- Mi J, Shaw AE, Pak CW, Walsh KP, Minamide LS, Bernstein BW, Kuhn TB, Bamberg JR (2013) A genetically encoded reporter for real-time imaging of cofilin-actin rods in living neurons. *PLoS One* 8:e83609.
- Miller MG, Shukitt-Hale B (2012) Berry fruit enhances beneficial signaling in the brain. *J Agric Food Chem* 60:5709-15.
- Minamide LS, Shaw AE, Sarmiere PD, Wiggan O, Maloney MT, Bernstein BW, Sneider JM, Gonzalez JA, Bamberg JR (2003) Production and use of replication-deficient adenovirus for transgene expression in neurons. *Methods Cell Biol* 71:387-416.
- Minamide LS, Striegl AM, Boyle JA, Meberg PJ, Bamberg JR (2000) Neurodegenerative stimuli induce persistent ADF/actin rods that disrupt distal neurite function. *Nat Cell Bio* 2:628-36.
- Mo GL, Li Y, Du RH, Dai DZ, Cong XD, Dai Y (2014) Isoproterenol induced stressful reactions in the brain are characterized by inflammation due to activation of NADPH oxidase and ER stress: attenuated by Apocynin, Rehmannia complex and Triterpene acids. *Neurochem Res* 39:719-30.
- Möller T (2010) Neuroinflammation in Huntington's disease. *J Neural Transm* 117:1001-8.

- Moore BD, Chakrabarty P, Levites Y, Kukar TL, Baine AM, Moroni T, Ladd TB, Das P, Dickson DW, Golde TE (2012) Overlapping profiles of A $\beta$  peptides in the Alzheimer's disease and pathological aging brains. *Alzheimers Res Ther* 4:18.
- Morgan TE, Lockerbie RO, Minamide LS, Browning MD, Bamburg JR (1993) Isolation and characterization of a regulated form of actin depolymerizing factor. *J Cell Biol* 122:623-33.
- Mortiboys H, Aasly J, Bandmann O (2013) Urocholic acid rescues mitochondrial function in common forms of familial Parkinson's disease. *Brain* 136:3038-50.
- Mrek RE, Griffin WS (2005) Potential inflammatory biomarkers in Alzheimer's disease. *J Alzheimers Dis* 8:369-375.
- Niwa R, Nagata-Ohashi K, Takeichi M, Mizuno K, Uemura T (2002) Control of actin reorganization by Slingshot, a family of phosphatases that desphosphorylate ADF/cofilin. *Cell* 108:233-46.
- Podlisny MB, Ostaszewski BL, Squazzo SL, Koo EH, Rydell RE, Teplow DB, Selkoe DJ (1995) Aggregation of secreted amyloid beta-protein into sodium dodecyl sulfate-stable oligomers in cell culture. *J Biol Chem* 270:9564-70.
- Orsucci D, Mancuso M, Ienco EC, Simoncini C, Siciliano G, Bonuccelli U (2013) Vascular factors and mitochondrial dysfunction: a central role in the pathogenesis of Alzheimer's disease. *Curr Neurovasc Res* 10:76-80.
- Pal R, Thakur PB, Li S, Minard C, Rodney GG (2013) Real-time imaging of NADPH oxidase activity in living cells using a novel fluorescent protein reporter. *PLoS One* 8:e63989.

- Persidsky Y, Ho W, Ramirez SH, Potula R, Abood ME, Unterwald E, Tuma R  
(2011) HIV-1 infection and alcohol abuse: neurocognitive impairment, mechanisms of neurodegeneration and therapeutic interventions. *Brain Behav Immun* 25:S61-70.
- Popik W, Alce TM, Au WC (2002) Human immunodeficiency virus type 1 uses lipid raft-colocalized CD4 and chemokine receptors for productive entry into CD4(+) cells. *J Virol* 76:4709-22.
- Pradines E, Loubet D, Mouillet-Richard S, Manivet P, Launay JM, Kellermann O, Schneider B (2009) Cellular prion protein coupling to TACE-dependent TNF $\alpha$  shedding controls neurotransmitter catabolism in neuronal cells. *J Neurochem* 110:912-23.
- Pradines E, Hernandez-Rapp J, Villa-Diaz A, Dakowski C, Ardila-Osorio H, Haik S, Schneider B, Launay JM, Kellermann O, Torres JM, *et al.* (2013) Pathogenic prions deviate PrP<sup>C</sup> signaling in neuronal cells and impair A-beta clearance. *Cell Death Dis* 4:e456.
- Prasad S, Yadav VR, Sung B, Reuter S, Kannappan R, Deorukhkar A, Diagaradjane P, Wei C, Baladandayuthapani V, Krishnan S, *et al.* (2012) Ursolic acid inhibits growth and metastasis of human colorectal cancer in an orthotopic nude mouse model by targeting multiple cell signaling pathways: chemosensitization with capecitabine. *Clin Cancer Res* 18:4942-53.
- Prusiner SB (2013) Biology and genetics of prions causing neurodegeneration. *Annu Rev Genet* 47:601-23.
- Pruta R, Furmuga-Jabłońska W, Maciejewski R, Ułamek-Kozioł M, Jabłoński M

- (2013) Brain ischemia activates  $\beta$ - and  $\gamma$ -secretase cleavage of amyloid precursor protein: significance in sporadic Alzheimer's disease. *Mol Neurobiol* 47:425-34.
- Renner M, Melki R (2014) Protein aggregation and prionopathies. *Pathol Biol* S0369-8114:0003-9.
- Roh SE, Woo JA, Lakshmana MK, Uhlar C, Ankala V, Boggess T, Liu T, Hong YH, Mook-Jung I, Kim SJ *et al.* (2013) Mitochondrial dysfunction and calcium deregulation by the RanBP9-cofilin pathway. *FASEB J* 27:4776-89.
- Rosi S, Pert CB, Ruff MR, Gann-Gramling K, Wenk GL (2005) Chemokine receptor 5 antagonist D-Ala-peptide T-amide reduces microglia and astrocyte activation within the hippocampus in a neuroinflammatory rat model of Alzheimer's disease. *Neurosci* 134:671-6.
- Ruff MR, Polianova M, Yang QE, Leoung GS, Ruscetti FW, Pert CB (2003) Update on D-ala-peptide T-amide (DAPTA): a viral entry inhibitor that blocks CCR5 chemokine receptors. *Curr HIV Res* 1:51-67.
- Rushworth JV, Hooper NM (2010) Lipid rafts: linking Alzheimer's amyloid- $\beta$  production, aggregation, and toxicity at neuronal membranes. *Int J Alzheimers Dis* 2011:603052.
- Santuccione A, Sytnyk V, Leshchyns'ka I, Schachner M (2005) Prion protein recruits its neuronal receptor NCAM to lipid rafts to activate p59fyn and to enhance neurite outgrowth. *J Cell Biol* 169:341-54.
- Sarmiere PD, Bamberg JR (2003) Regulation of the neuronal actin cytoskeleton by ADF/cofilin. *J Neurobiol* 58:103-17.

- Scheff SW, Neltner JH, Nelson PT (2014) Is synaptic loss a unique hallmark of Alzheimer's disease? *Biochem Pharmacol* 88:517-28.
- Schmitt-Ulms G, Legname G, Baldwin MA, Ball HL, Bradon N, Bosque PJ, Crossin KL, Edelman GM, DeArmond SJ, Cohen FE, Prusiner SB (2001) Binding of neural cell adhesion molecules (N-CAMs) to the cellular prion protein. *J Mol Biol* 314:1209-25.
- Schneider B, Mutel V, Pietri M, Ermonval M, Mouillet-Richard S, Kellermann O (2003) NADPH oxidase and extracellular regulated kinases 1/2 are targets of prion protein signaling in neuronal and nonneuronal cells. *Proc Natl Acad Sci USA* 100:13326-31.
- Schönhofen P, de Medeiros LM, Chatain CP, Bristot IJ, Klamt F (2014) Cofilin/actin rod formation by dysregulation of cofilin-1 activity as a central initial step in neurodegeneration. *Mini Rev Med Chem* 14:393-400.
- Seidl SE, Santiago JA, Bilyk H, Potashkin JA (2014) The emerging role of nutrition in Parkinson's disease. *Front Aging Neurosci* 6:36.
- Serrano F, Kolluri NS, Wientjes FB, Card JP, Klann E (2003) NADPH oxidase immunoreactivity in the mouse brain. *Brain Res* 988:193-8.
- Shaw AE, Minamide LS, Bill CL, Funk JD, Maiti S, Bamberg JR (2004) Cross-reactivity of antibodies to actin-depolymerizing factor/cofilin family proteins and identification of the major epitope recognized by a mammalian actin-depolymerizing factor/cofilin antibody. *Electrophoresis* 25:2611-20.
- Shih YH, Chein YC, Wang JY, Fu YS (2004) Ursolic acid protects hippocampal neurons against kainite-induced excitotoxicity in rats. *Neurosci Lett* 362:136-40.

- Shukkit-Hale B, Lau FC, Joseph JA (2008) Berry fruit supplementation and the aging brain. *J Agric Food Chem* 56:636-41.
- Sivanandam TM, Thakur MK (2012) Traumatic brain injury: a risk factor for Alzheimer's disease. *Neurosci Biobehav Rev* 36:1376-81.
- Socci DJ, Pert CB, Ruff MR, Arendash GW (1996) Peptide T prevents NBM lesion-induced cortical atrophy in aged rats. *Peptides* 17:831-7.
- Sorce S, Krause KH, Jaquet V (2012) Targeting NOX enzymes in the central nervous system: therapeutic opportunities. *Cell Mol Life Sci* 69:2387-404.
- Spencer JPE (2010) The impact of fruit flavonoid on memory and cognition. *Brit J Nutr* 104:S40-47
- Stahl N, Baldwin MA, Hecker R, Pan KM, Burlingame AL, Prusiner SB (1992) Glycosylinositol phospholipid anchors of the scrapie and cellular prion protein contains sialic acid. *Biochemistry* 31:5043-53.
- Sudduth TL, Schmitt FA, Nelson PT, Wilcock DM (2013) Neuroinflammatory phenotype in early Alzheimer's disease. *Neurobiol Aging* 34:1051-9.
- Sumimoto H (2005) Roles and activation mechanisms of Nox family oxidases in animals. *Tanpakushitsu Kakusan Koso* 50:302-9.
- Sun AY, Wang Q, Simonyi A, Sun GY (2008) Botanical phenolics and brain health. *NeuroMusc Med* 10:259-74.
- Sun HQ, Kwiatkowska K, Yin HL (1995) Actin monomer binding proteins. *Curr Biol* 7:102-10.
- Sweeney MI, Kalt W, MacKinnon SL, Ashby J, Gottschall-Pass T (2002) Feeding

- rats diets enriched in lowbuck blueberries for six weeks decreases ischemia-induced brain damage. *Nutr Neurosci* 5:627-31.
- Szarc vel Szic K, Ndlovu MN, Haegeman G, Berghe WV (2010) Nature or nurture: let food be your epigenetic medicine in chronic inflammatory disorders. *Biochem Pharm* 80:1816-32.
- Thies E, Mandelkow EM (2007) Missorting of tau in neurons causes degeneration of synapses that can be rescued by the kinase MARK2/Par-1. *J Neurosci* 27:2896-907.
- Thinakaran G, Koo EH (2008) Amyloid precursor protein trafficking, processing, and function. *J Biol Chem* 283:29615-9.
- Um JW, Kaufman AC, Kostylev M, Heiss JK, Stagi M, Takahashi H, Kerrisk ME, Vortmeyer A, Wisniewski T, Koleske AJ, Gunther EC, Nygaard HB, Strittmatter SM (2013) Metabotropic glutamate receptor 5 is a coreceptor for Alzheimer  $\alpha\beta$  oligomer bound to cellular prion protein. *Neuron* 79:887-902.
- Um JW, Nygaard HB, Heiss JK, Kostylev MA, Stagi M, Vortmeyer A, Wisniewski T, Gunther EC, Strittmatter SM (2012) Alzheimer amyloid- $\beta$  oligomer bound to postsynaptic prion protein activates Fyn to impair neurons. *Nat Neurosci* 15:1227-35.
- Vallet P, Charnay Y, Steger K, Ogier-Denis E, Kovari E, Herrmann F, Michel JP, Szanto I (2005) Neuronal expression of the NADPH oxidase NOX4, and its regulation in mouse experimental brain ischemia. *Neuroscience* 132:223-8.
- Vilhardt F, Van Deurs B (2004) The phagocyte NADPH oxidase depends on cholesterol-enriched membrane microdomains for assembly. *EMBO J* 23:739-48.

- Vural P, Değirmencioğlu S, Parildar-Karpuzoğlu H, Dođru-Abbasođlu S, Hanagasi HA, Karadađ B, Gürvit H, Emre M, Uysal M (2009) The combinations of TNF $\alpha$ -308 and IL-6 -174 or IL-10 -1082 genes polymorphisms suggest an association with susceptibility to sporadic late-onset Alzheimer's disease. *Acta Neurol Scand* 120:396-401.
- Walsh KP, Minamide LS, Kane SJ, Shaw AE, Brown DR, Pulford B, Zabel MD, Lambeth JD, Kuhn TB, Bamburg JR (2014) Amyloid- $\beta$  and proinflammatory cytokines utilize a prion protein-dependent signaling pathway to activate NADPH oxidase and induce cofilin-actin rods in hippocampal neurons. *PLoS One* 9:e95995.
- Wang Y, Shibasaki F, Mizuno K (2005) Calcium signal-induced cofilin dephosphorylation is mediated by Slingshot via calcineurin. *J Biol Chem* 280:12683-9.
- Wang YJ, Lu J, Wu DM, Zheng ZH, Zheng YL, Wang XH, Ruan J, Sun X, Shan Q, Zhang ZF (2011) Ursolic acid attenuates lipopolysaccharide-induced cognitive deficits in mouse brain through suppressing p38/NF- $\kappa$ B mediated inflammatory pathways. *Neurobiol Learn Mem* 96:156-65.
- Whiteman IT, Gervasio OL, Cullen KM, Guillemin GJ, Jeong EV, Witting PK, Antao ST, Minamide LS, Bamburg JR, Goldsberry C (2009) Activated actin-depolymerizing factor/cofilin sequesters phosphorylated microtubule-associated protein during the assembly of alzheimer-like neuritic cytoskeletal striations. *J Neurosci* 29:12994-3005.
- Wilkinson K, Boyd JD, Glicksman M, Moore KJ, El Khoury J (2011) A high

- content drug screen identifies ursolic acid as an inhibitor of amyloid beta protein interactions with its receptor CD36. *J Biol Chem* 286:34914-34922.
- Willmann R, Pun S, Stallmach L, Sadasivam G, Santos AF, Caroni P, Fuhrer C (2006) Cholesterol and lipid microdomains stabilize the postsynapse at the neuromuscular junction. *EMBO J* 25:4050-60.
- Wilson RS, Mendes De Leon CF, Barnes LL, Schneider JA, Bienias JL, Evans DA, Bennett DA (2002) Participation in cognitively stimulating activities and risk of incident Alzheimer disease. *JAMA* 287:742-8.
- Wu DM, Lu J, Zhang YQ, Zheng YL, Hu B, Cheng W, Zhang ZF, Li MQ (2013) Ursolic acid improves domoic acid-induced cognitive deficits in mice. *Toxicol Apply Pharmacol* 271:127-36.
- Yang B, Rizzo V (2007) TNF-alpha potentiates protein-tyrosine nitration through activation of NADPH oxidase and eNOS localized in membrane rafts and caveolae of bovine aortic endothelial cells. *Am J Physiol Heart Circ Physiol* 292:H954-62.
- Yang SH, Gangidine M, Pritts TA, Goodman MD, Lentsch AB (2013) Interleukin 6 mediates neuroinflammation and motor coordination deficits after mild traumatic brain injury and brief hypoxia in mice. *Shock* 40:471-5.
- Yonezawa N, Homma Y, Yahara I, Sakai H, Nishida E (1991) A short sequence responsible for both phosphoinositide binding and actin binding activities of cofilin. *J Biol Chem* 266:17218-21.
- Yoshiyama Y, Uryu K, Higuchi M, Longhi L, Hoover R, Fujimoto S, McIntosh T,

- Lee VM, Trojanowski JQ (2005) Enhanced neurofibrillary tangle formation, cerebral atrophy, and cognitive deficits induced by repetitive traumatic brain injury in a transgenic tauopathy mouse model. *J Neurotrauma* 22:1134-41.
- You H, Tsutsui S, Hameed S, Kannanayakal TJ, Chen L, Xia P, Engbers JD, Lipton SA, Stys PK, Zamponi GW (2012) A $\beta$  neurotoxicity depends on interactions between copper ions, prion protein, and N-methyl-D-aspartate receptors. *Proc Natl Acad Sci USA* 109:1737-42.
- Zang LL, Wu BN, Lin Y, Wang J, Fu L, Tang ZY (2014) Research progress of ursolic acid's anti-tumor actions. *Chin J Integr Med* 20:72-9.
- Zhou L, Ding Y, Chen W, Zhang P, Chen Y, Lv X (2013) The in vitro study of ursolic acid and oleanolic acid inhibiting cariogenic microorganisms as well as biofilm. *Oral Dis* 19:494-500.
- Zhou L, Saksena NK (2013) HIV associated neurocognitive disorders. *Infect Dis Rep* 5:e8.
- Zhu X, Owen JS, Wilson MD, Li H, Griffiths GL, Thomas MJ, Hiltbold EM, Fessler MB, Parks JS (2010) Macrophage ABCA1 reduces MyD88-dependent Toll-like receptor trafficking to lipids rafts by reduction of lipid raft cholesterol. *J Lipid Res* 51:3196-2.